Evaluating multi-satellite Chlorophyll-a datasets

An ocean colour case study within the Southern Benguela

Craig Oehley

Department of Oceanography

University of Cape Town

Rondebosch, Cape Town

South Africa

Supervisor

M **Smith**, CSIR

Co-supervisor

C **Whittle**, CSIR

February 2025

MSc dissertation submitted in partial fulfilment of the requirements for the degree of Master of Science by

coursework and dissertation in Applied Ocean Sciences through the Marine and Antarctic Research centre for Innovation and Sustainability (MARiS)

Declaration

I, Craig **Oehley** hereby:

1. Grant the University of Cape Town free licence to reproduce the above thesis in whole or in part, for the purpose of research;

2. Declare that:

   (a) This thesis is my own unaided work, both in concept and execution, and apart from the normal guidance from my supervisors, I have received no assistance except as stated in my bibliography and acknowledgements.

   (b) Neither the substance nor any part of the above thesis has been submitted in the past, or is being, or is to be submitted for a degree at this University or at any other university.

Signed by candidate

Craig **Oehley**

Department of Oceanography

University of Cape Town

Fri 14 February, 2025

Acknowledgements

I would like to acknowledge my supervisors Dr Marie Smith and Mr Christo Whittle for taking time out of their careers to advise, support, and encourage the production of this thesis, as well as going the extra mile to provide external opportunities for research and growth. Their open but professional attitude's allowed this thesis to progress in a natural, smooth manner, and I'm truly grateful. I'd additionally like to express thanks to Dr Louise Gammage and Prof Marcello Vichi for organising and operating the exceptional Applied Ocean Science Masters course. This program has introduced me to an inspiring field of work that I would not have discovered otherwise. Finally, a warm thank you to my family for believing in my vision and supporting this journey.

Abstract

Chlorophyll-a (chl-a), a photosynthetic pigment that can be estimated from satellite ocean colour, is often used as a proxy for phytoplankton biomass and to derive primary productivity. Initiatives such as the Ocean Colour Climate Change Initiative (OC-CCI) produce merged multi-satellite products to create consistent, long-term time-series datasets for climate studies at a global scale. Their ability to handle variable in-water conditions is critical for their mission parameters. This study compares the performance of two European multi-satellite chl-a products, from the OC-CCI and GlobColour projects against a regionally tuned Sentinel-3 product within the Southern Benguela region. The three products were assessed against a collated database of coincident in situ chl-a matchups to derive a series of performance metrics. The regionally tuned Sentinel-3 product outperformed the two global products in terms of Mean Absolute Error but showed a slight, consistent overestimation bias. Analysis of match-ups showed an underestimation of high chl-a concentrations and overestimation of lower chl-a concentrations by both global products. An application of the products within St Helena bay during high biomass bloom events showed that the Sentinel-3 product's ability to capture extreme chl-a concentrations was far higher than both global products. Spatial mismatch between zones of high chl-a concentration also indicate differences in processing chains and flagging techniques.

Contents

List of Figures

List of Tables

Glossary

Acronyms	Description
chl-a	Chlorophyll-a
CMEMS	Copernicus Marine Service
CZCS	Coastal Zone Colour Sensor
ECV	Essential Climate Variable
ESA	European Space Agency
GlobColour	Global Ocean Colour
KDE	Kernal Density Estimate
MAE	Mean Absolute Error
MERIS	Medium Resolution Imaging Spectrometer
MODIS	Moderate Resolution Imaging Spectroradiometer
OC-CCI	Ocean Colour-Climate Change Initiative
OLCI	Ocean and Land Colour Instrument
R_{rs}	Remote Sensing Reflectance
RMSE	Root Mean Square Error
SeaWiFS	Sea-viewing Wide Field-of-view Sensor
VIIRS	Visible Infrared Imaging Radiometer Suite

Table 1: Table of Acronyms and Abbreviations used throughout the paper

Chapter 1

Introduction

1.1 Background

The scientific study of climate change has revealed changes in short-term ecosystem variability and long term changes in ecosystem characteristics. There is a consistent need for long-term data collection and acquisition of climate variables to best understand and account for potential natural variability versus anthropogenic induced change. The Global Climate Observation System (GCOS) co-founded in 1992 by World Meteorological Organization (WMO), Intergovernmental Oceanographic Commission (IOC) of United Nations Educational, Scientific and Cultural Organization (UNESCO), United Nations Environment Programme (UNEP), and International Council for Science (ISC), has the express goal of ensuring that appropriate observations and information can be obtained and collected for the scientific community and policy makers to address climate-related issues. GCOS identified a selection of *essential climate variables* (ECV) which require long-term data collection to address future climate issues, one of which, is ocean colour (Mason et al., 2010). The term ocean colour includes water leaving radiances, as well as derived chlorophyll-a (chl-a) concentrations and other marine biogeochemical properties.

Ocean colour work is most commonly used to quantify the concentration of chl-a, which can be used as an indicator of phytoplankton biomass, due to its ubiquity in photosynthetic organisms. Phytoplankton take up atmospheric Carbon Dioxide (CO_2) and convert it into organic carbon, playing a critical role in the global carbon cycle. The extent of this carbon fixing is estimated to rival that of all terrestrial primary production (Field et al., 1998). Moreover, phytoplankton represent the base of almost all marine food webs from the open ocean to the coastal seas. Therefore, the monitoring of such organisms allows us to link the effects of phytoplankton on the climate system as well as the effects of climate change on the marine biosphere. Due to the key role of phytoplankton in the global carbon cycle, the need to detect and quantify its biomass and variability on a global scale has long been recognised. Satellite derived observations help to create large-scale databases of chl-a, both on a spatial, and temporal basis. Climate and earth observation satellites used to collect ocean colour data can cover enormous swathes of space. The Ocean Land Colour Instrument (OLCI) flown on board the European Space Agency's (ESA) Sentinel-3 satellites allow for global coverage on a

near-daily basis. In order to monitor global oceanic and climate trends that can have natural variation on large spatial and temporal scales, satellites observations have become invaluable. Moreover, the combination of multiple satellite missions and databases, each spanning multiple years, to form a coherent time-series provides an even better capability to detect these large-scale climate diagnostic trends (Yu et al., 2023). Examples of these multi-satellite database initiatives include the Ocean colour Climate Change Initiative (OC-CCI), funded by the ESA (Sathyendranath et al., 2019).

1.2 Study Rational and Objectives

As a region of extremely high productivity, the Benguela current represents an area of significance for marine science and industry. With chl-a concentrations reaching >100 mg m^{-3} in some circumstances, the productivity of this coastal region plays an important ecological and economic role. Thus the ability to correctly quantify and monitor chl-a concentrations within this region is of interest to the marine scientific community. Extensive and intense seasonal upwelling result in high nutrient loads in surface waters that promote the occurrence of high biomass blooms and other potentially harmful algae blooms (HABs) in the Benguela region (Pitcher and Probyn, 2016). These can have devastating effects on the surrounding ecosystems, threatening not just biodiversity but many economically important industries such as fisheries or marine aquaculture (Ndhlovu et al., 2017; van der Lingen et al., 2016). The Benguela offers a unique system in terms of optical properties. Despite containing large volumes of phytoplankton and therefore chl-a concentrations, the region typically does not contain other highly scattering inorganic particles normally associated with coastal regions of high productivity. However, the high phytoplankton biomass poses challenges for traditional ocean colour remote sensing techniques, which led to the development of a regional algorithm more suited to local conditions (Smith et al 2018).

While the generation of global datasets (such as the OC-CCI) serves to build consistent and long-term data, the algorithms used by global datasets and employed to produce derived geophysical products might not accurately represent niche conditions found in particular regions. Dataset developers have implemented methods to effectively characterize known bodies of water and apply the most suitable algorithms. However, these methods can differ significantly from one database to another. In order to evaluate the ability of global datasets to handle temporal and spatial variability, it is beneficial for them to be applied to regions that experience both. The diverse conditions of the Benguela, influenced both temporally by seasonal upwelling and spatially by its coastal gradient, make it an ideal testing ground for global datasets.

The key questions asked in this study are as follows:

1) **To what extent can global multi-satellite datasets correctly and appropriately classify chl-a concentrations within the Southern Benguela?** This will be done by comparing their products directly to both in situ measurements as well as the recently developed algorithm for this region. The comparison

of algorithm performance will be done via multiple statistical metrics. Thanks to its naturally high chl-a concentration variability, the Benguela system represents a useful system to test the ability of these global datasets to handle a variety of conditions, something that is critical to their mission objective in estimating consistent results for climate-based research and analysis.

2) **How effective are the various datasets in capturing chl-a concentration ranges and spatio-temporal variability?** This case study will focus on monitoring the performance of global multi-satellite datasets in detecting high biomass blooms in the St Helena Bay. High biomass blooms within this region can often be associated with HABs. The ability to detect such blooms will be an asset for global data sets, and their ability to do so can be appropriately compared in this region.

Chapter 2

Literature review

2.1 Phytoplankton, Chlorophyll-a and nutrients

Phytoplankton, coming from the latin words for light "*phyton*" and wanderer "*planktos*", is a functional group of organisms, commonly too small to view with the naked eye. Phytoplankton cover a broad range of organisms including coccolithophorids, diatoms, dinoflagellates and prasinophytes among others (Collins et al., 2014). Phytoplankton can be classified ubiquitously as photoautotrophs. *Photo* indicating their source of energy as light, and *autotrophs* referring to their ability to generate organic carbon from the inorganic compounds around them. A key component to the success of photosynthesis, the process in which all phytoplankton use light to create energy, is the use of photosynthetic pigments. These are biological substances with specific absorption properties, leading to the reflection or scattering of selective colours. Chl-a is the most common photosynthetic pigment, and is ubiquitous in phytoplankton. Photosynthesis results in the taking up of CO_2, and the subsequent conversion of inorganic carbon into organic biomass. As CO_2 gets taken up from the water through photosynthesis, it facilitates the drawdown of CO_2 from the atmosphere to match equilibrium. As phytoplankton decay or are consumed, a small portion of their organic biomass reaches the ocean floor, sequestered away. This net removal of CO_2 from the ocean-atmosphere system is often referred to by oceanographers as the the biological pump, and is a critical process in the earths carbon cycle.

In the majority of marine conditions, the most important nutrients required for phytoplankton are nitrogen, phosphorous, silicon, and iron. The 1958 paper by oceanographer Redfield detailed the consistent ratio of carbon, nitrogen and phosphorous that phytoplankton compose their biomass out of (Redfield, 1958). Whilst phytoplankton obtain their carbon naturally through photosynthesis, Redfield's ratio revealed the critical reliance of phytoplankton on nitrogen and phosphorous. In the vast majority of the ocean however, there is an observed lack of adequate nutrients for phytoplankton production (Moore et al., 2013).

As photoautotrophs, phytoplankton depend on sunlight for their source of energy. However, the density and molecular structure of water limits light penetration, with the majority being either absorbed or scattered. This restricts photoautotrophs to the uppermost layer of the ocean referred to as the euphotic zone, where

sufficient sunlight is provided for photosynthesis to be possible. This creates a challenge for phytoplankton, which naturally move nutrients out of the surface water and into the deep ocean through the biological pump. In the open ocean, the natural and biogeochemical inputs of nutrients such as nitrogen into the surface water does not replenish the rate at which it's exported by the biological pump. The vast majority of the open ocean is classified as oligotrophic with chl-a concentrations typically ranging from 0.1 - 0.5 mg m^{-3} (Yasunaka et al., 2022; Hu et al., 2012).

In some coastal regions however, where strong upwelling of deep water occurs, a temporary supply of excess nutrients can become available within the euphotic zone. This is naturally followed by an increased growth-rate and biomass of phytoplankton within the region, associated with similarly higher concentrations of chl-a within the water column. In regions such as the Southern Benguela, these chl-a concentrations can reach far beyond 200 mg m^{-3} (Pitcher and Nelson, 2006).

2.2 Benguela region

The Benguela current is an eastern boundary current running equator-ward along the western coast of Southern Africa. As an eastern boundary current, it features typically cold, productive waters, with a closer, warm, poleward moving jet inshore. The current itself forms part of the Benguela upwelling system which extends north into Namibia and Angola, and is a region of high primary production variability which is strongly linked to upwelling events and cycles. The Southern Benguela falls within the larger Benguela upwelling system, and is typically defined from Luderitz to Port Alfred. As such, it comprises of South Africa's west coast, wrapping around Cape Point and extending far along the South coast. A combination of low-pressure cells trapped against the coast, the region's shelf width, and topography help create distinct upwelling zones, in addition to pulsed upwelling events often ranging from 3 to 10 days in interval (Hutchings et al., 2009). It's these conditions that help bring up cold, nutrient rich water, and fuel ideal conditions for phytoplankton growth. Trends in regional productivity reveal both short term variability, which tracks individual upwelling events, and longer term seasonal variability associated with seasonal winds, such as the South Easterly (Hutchings et al., 2009). The distinct pulsed nature of upwelling in the Benguela system creates periods of quiescence between active upwelling events, allowing phytoplankton biomass to increase rapidly in ideal sea state conditions enriched by excess nutrients available. This effect can become even stronger in bays such as St Helena bay, where hydrographic retention keeps nutrients concentrated and reduces the flushing rate for both phytoplankton and nutrients (Pitcher and Nelson, 2006).

2.3 Ocean colour processes

2.3.1 Ocean optics

The broad objective of remote sensing ocean colour is to quantify and identify substances in the ocean from the changes in spectral shape and magnitude of the water leaving light signal. These changes are caused by optically active constituents, substances which contribute to the optical properties of water, such as phytoplankton or sediment. This requires an understanding of the physical interactions and descriptions of light, the study of radiometry. When light interacts with a medium or matter, one of three scenarios may occur; absorption, inelastic scattering or elastic scattering. The absorption and scattering properties of a medium are known as it's Inherent Optical Properties (IOP). Since these properties are a function of the medium and material inside the medium, they are independent of light itself. IOPS can be broken down into two broad fundamental terms, *absorption coefficient* which describes the quality in which a medium absorbs light, and the *volume scattering function* which describes the quality in which a medium scatters light. They can be measured via a variety of experiments and processes, a brief summary of which can be found in Mobley (2022). The total IOPs for a body of water can be determined from the sum of IOPs for each individual component, such that total absorption in a simplified hypothetical water body can be classified for example as

$$\alpha_{\text{total}} = \alpha_{\text{water}} + \alpha_{\text{phytoplankton}} \tag{2.1}$$

Whilst IOPs offer an exhaustive and ideal method for quantifying the optical properties of a water body, it remains a largely impracticable solution even with modern technology. The expense of equipment required for generating IOPs is one barrier to entry, another is the acquisition of the water samples, and finally is the expertise required to carry out the experiments. An alternative approach is to measure the Apparent Optical Properties (AOP) of a water body. By definition, AOPs are properties which are generated from the IOPs within the water as well as the distribution of radiance within the water i.e. AOPs are directly dependent on light as a variable. Since AOPs are dependent on light, they are naturally influenced by variable external conditions such that AOPs generated on a cloudy day will differ from those generated on a clear day. Most AOPs are taken as either derivates of radiance/irradiance or ratios (reflectances). These transformations help reduce the variability caused by external conditions whilst maintaining sensitivity to the IOPs.

The relationship between IOPs and AOPs is described by radiative transfer , which is the description of light through the medium. Radiative transfer equations are a set of equations with varying degrees of complexity used to navigate from IOPs to AOPs (Fig 2.1). These equations are two-point boundary problems since

radiance values need to be calculated at both the start and end point of the medium (ocean or atmosphere). Due to their complexity, radiative transfer equations require strong numerical methods for solving.

Determining radiometric measurements such as radiance and reflectance as a function of substances within the water is known as the forward problem. This problem can be thought of as a 'solved problem', in the sense that, the accuracy of the calculated radiance is only limited by the specifications of the IOPs and light field. With the appropriate time and resources required to determine IOPs, and enough computing power required to solve the numerical radiative transfer equation, we would arrive at perfect AOP values.

Ocean colour and remote sensing however, is the inverse problem, attempting to use radiometric measurements to determine IOPs, and thus the substances responsible for generating them (Fig 2.1). These radiometric measurements not only fall short of describing the full distribution of radiance, but are also prone to error through incorrect instrument calibration or erroneous atmospheric correction (see 2.3.2).

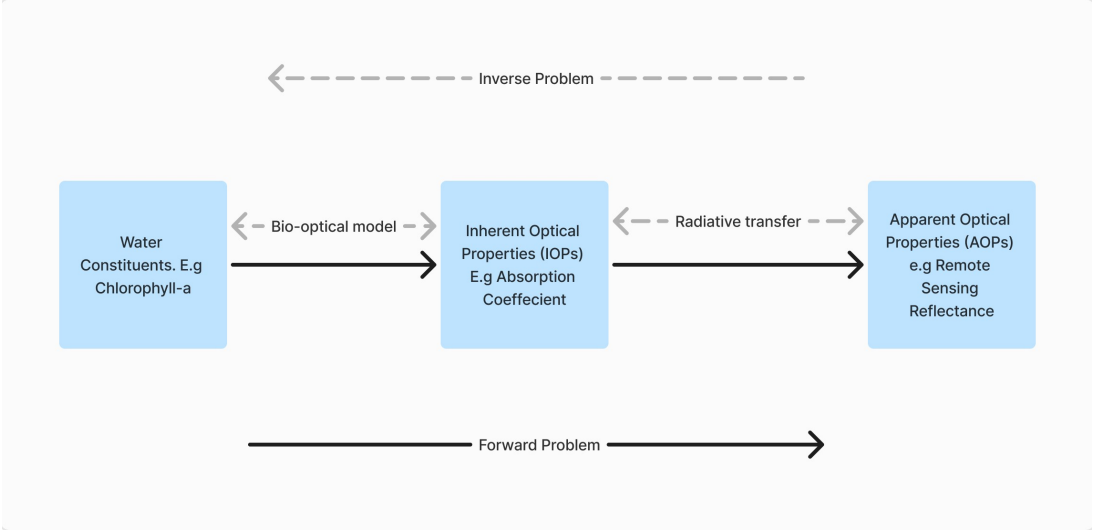

Figure 2.1: Ocean optical properties, and their relationships.

The radiometric quantities and AOPs that satellites calculate are formulated to minimize the influence of the light field itself whilst maintaining the sensitivity to the inherent optical properties within the water. However, two different sets of IOPs with two correspondingly different light fields could potentially generate the same values which our satellites measure. This problem is known as the *uniqueness of the solution*. It's important to recognise these constraints, as they are key to the philosophy behind passive remote sensing, it's for this reason that products such as chl-a are given as *estimates*. In modelling these outputs, we are attempting to relate what is already known about these quantities to what limited information is being received by our sensors. Nevertheless, despite these known constraints and flaws, various algorithms used within the inversion process aim to minimize and account for these problems, to best deliver large amounts of quantitative information about ocean colour without which, there would be no replacement.

2.3.2 Atmospheric correction

The pipeline of information to derive ocean colour products consists of multiple steps, each with different possible methods and variations. The total radiance received by a sensor on board an earth observation satellite L_{u} also known as Top Of Atmosphere (TOA) radiance can be broken down into three sources of signal: the atmosphere, the ocean surface, and the ocean water column (Mobley, 2022), such that

$$L_u = L_a + L_r + L_w \tag{2.2}$$

The atmospheric signal L_{a} is a result of solar radiance scattered by atmospheric components into the instrument. The ocean surface signal L_{r} is a result of solar radiance directly reflected by the water surface. Both of these sources of signal need to be removed in order to start analysing ocean colour, which can be found in the water leaving radiance from the ocean water column L_{w}. For this reason, an atmospheric correction algorithm is applied to best eliminate atmospheric and water reflectance signal. Figure 2.2 shows an example of how proportionally the atmospheric and surface-reflected signals contribute to the TOA radiance. Often the water leaving signal only accounts for 10 or less percent of the TOA radiance, hence the quality of the atmospheric correction algorithm/process can heavily impact the accuracy of the resulting product.

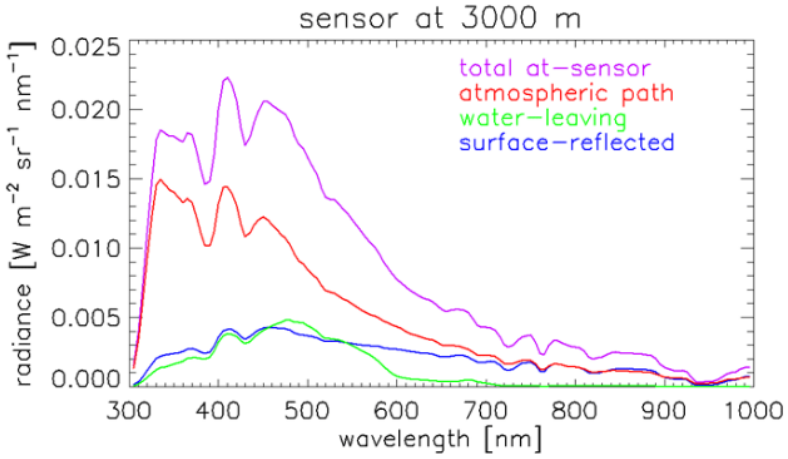

Figure 2.2: A partitioned radiance curve showing components resulting in TOA radiance at 3000m, generated by simulation software (Mobley, 2022)

In order to correctly apply atmospheric correction, the mechanisms behind these contributions need to be identified, isolated, and then corrected for. A more in depth version of equation 2.2 can be built. The atmospheric signal L_{a} can be broken down into Rayleigh radiance L_{R} , caused by atmospheric molecules smaller than the wavelengths of light, and aerosol contribution L_{A}, caused by the scattering of aerosol particles, as well as the multiple scattering from both aerosol and atmospheric molecules. The ocean surface

signal L_{r} can be broken down into contribution from ocean white caps L_{wc}, and sun glint L_g.

$$L_u = L_R + L_A + TL_g + tL_{wc} + tL_w \tag{2.3}$$

Note the addition of the terms T and t, these represent direct and diffuse transmittance respectively. Since all ocean properties are technically measured leaving the ocean surface, these terms represent the portion of radiance which reaches the top of the atmosphere to become TOA radiance.

Water leaving radiance L_{w} still however, contains elements affected by the viewing angle, solar zenith angle, atmospheric conditions and oceanic conditions at the time and place of information collection. The ideal situation would be an AOP that relies on none of these effects and that can be used at any time and space to represent that particular water body. To do this, the water leaving radiance needs to be normalized. The direct equation representing normalization require expressions not yet covered and unnecessary for the sake of this study, however in summary, the normalized water-leaving reflectance can be obtained by multiplying Remote Sensing Reflectance (R_{rs}) by π and *vice versa*. The role of atmospheric correction should not be overlooked, and constant improvements can mark significant benefits to ocean colour work, such as increasing observation capacity by removing sun glint patterns in sub-tropics (Steinmetz et al., 2011).

The final step for obtaining a usable radiometric value is *vicarious calibration*. Instead of a perfect mathematical model, ocean colour can be thought of as a form of statistical modelling. Following this analogy, vicarious calibration represents the error term, attempting to best fit our final modelled response to the 'truth' value. There is acknowledgement that despite the variety of techniques used, there will undoubtable be differences in the normalised water leaving radiance obtained by the satellite, and the actual water leaving radiance from the surface of the ocean (which is the truth value we are attempting to measure). Vicarious calibration involves using techniques to force the received satellite radiometric values closer to the water leaving radiance values from the surface of the ocean. This is achieved in two different methods: 1) a collection of in situ water leaving radiance values are used for match-up analysis against the satellite measured value; 2) a simulated set of TOA radiance results are generated that represent the ideal values the sensor should pick up under a given set of conditions, which are then compared to the measured signal for the same set of conditions for match-up analysis. In both cases, a correction factor is obtained via the match-up analysis and applied to the atmospheric correction process.

2.3.3 In-water Algorithms

The resulting Remote Sensing Reflectance (R_{rs}) represents the portion of solar radiation which is upwelled from the sea surface after interacting with the optically active components in the water as well as the water itself. The water leaving radiance in most natural bodies of water is influenced by three components outside

of the water itself: Phytoplankton, Suspended inorganic material and Yellow substances (coloured, dissolved organic substances as well as detrital particulate matter). Once the ocean colour signal has been isolated and water-leaving radiation determined, in-water algorithms (algorithms that work to estimate and account for constituents in the water column) are used to translate the R_{rs} into estimates of ocean colour components such as the chl-a pigment. No single algorithm can however, account for the multitude and variance of ocean signals that are produced on a global scale. To better classify this variation, two water cases are described (Morel and Gordon, 1983).

Case-1 waters which often include the open ocean, are influenced optically by water and phytoplanktonic constituents. Case-2 waters by contrast are optically influenced by suspended materials and yellow substances as well as phytoplankton. These definitions are based on functionality, Case-1 waters can, and often do, feature other substances and organisms other than phytoplankton which contribute to optical properties, however the contributions by these additions are small and can be modelled as a function of phytoplankton concentration IOCCG (2000). In Case-2 waters, these additional substances are: a) in large enough quantities to contribute significantly to optical properties, and b) found in independent concentrations from phytoplankton and not as a function of. Specific oceanic properties will be discussed further in the context of the study region.

Different approaches to ocean colour processing are required to handle these different cases. Case-1 waters typically exhibit negligible water leaving radiance in the near-infrared (NIR) region, thus a spectral band at this region is used to quantify the optical characteristics of the atmospheric signal which is extrapolated to the visible light spectrum. This is then used in part of the atmospheric correction process (Section 2.3.2). The optical properties of Case-1 waters show strong signals in the blue-green spectral region, a type of in-water algorithm called an *empirical* algorithm is often applied to them, which uses the ratio of R_{rs} in the blue and green bands to infer estimates of constituents such as chl-a. Empirical algorithms base their conversion ratios on pre-existing information and observations regarding the relationship between R_{rs} and chl-a concentrations, hence the name 'empirical'. Examples of these blue-green band ratio algorithms include the Ocean Colour (OC) suite of algorithms (O'Reilly and Werdell, 2019).

Unlike Case-1 waters, the multitude of optically influencing substances in Case-2 waters requires the analysis of multiple variables within the spectral signal, thus the need for more bands to be considered. As productivity and inorganic backscattering from substances such as sediment increase, the signal from the blue-green region becomes less reliable for chl-a quantification, leading to empirical algorithms that instead use reflectance features in the NIR (e.g. Gitelson et al. (2010)). Case-2 conditions may also lead to increased reflectance in the NIR due to high concentrations of scattering components, which poses a problem for the usual atmospheric correction algorithm used in Case-1 waters.

The complexity of Case-2 waters has also spurred the creation of an entirely different suite of algorithms, *Semi-analytical algorithms*. In summary, these algorithms use bio-optical models to relate the constituents of

the water body (such as phytoplankton) into IOPs, and radiative transfer models to simulate the subsequent AOPs. Examples of semi-analytical algorithms include the Quasi-Analytical Algorithm (QAA) (Lee et al., 2002) and NASA's Generalized Ocean Color Inversion Model (GIOP) (Werdell et al., 2013). The models simulate radiometric values for a variety of water constituents and concentrations, creating a mapping of the results. This map is then inversed to create an algorithm that uses radiometric values to determine the water constituents. Fig 2.3 shows the philosophical differences when compared against empirical algorithms.

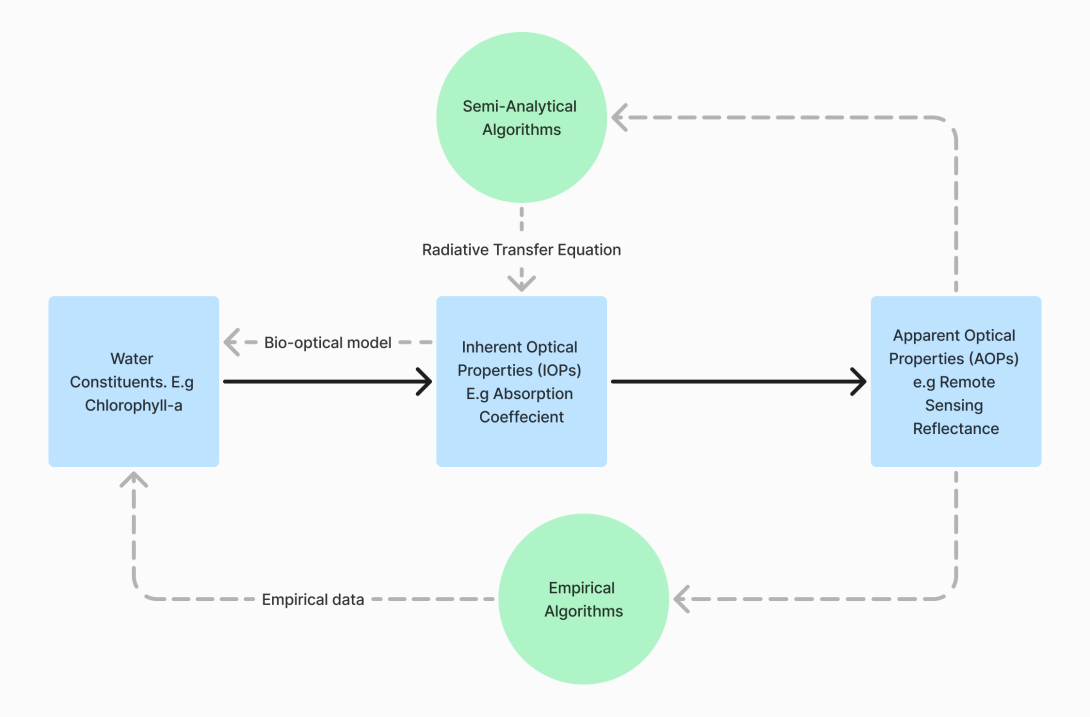

Figure 2.3: Differing pathways taken by empirical and semi-analytical algorithms

A common step for deriving chl-a concentrations in the modern ocean colour era includes the switching and weighting of multiple algorithms based on certain flags and thresholds (Hu et al., 2012), the goal being a seamless switch between different algorithms for the various conditions and signals being picked up. This is increasingly necessary a) in regions of naturally high chl-a variability b) when attempting to build large spatial and temporal databases that are prone to large amounts of variation due to scale. This concept is elaborated further in the following section.

2.4 Remote sensing within the Benguela

Ocean colour remote sensing started with the launch of the first ocean colour sensor, the Coastal Zone Colour Sensor (CZCS) in 1978, and subsequently along with it, estimations of chl-a concentrations (Gordon et al., 1980). Examples of ocean colour work being performed in the Benguela region date back to the CZCS. Studies were conducted that produced works detailing the validity of remote sensing results (Shannon et al., 1984) , inter-annual and seasonal variability of chl-a concentrations (Villiers, 1998), and the relationships between Sea Surface Temperature (SST) and chl-a. Technical details of these works are not given since

whilst the theoretical principles of Ocean colour work are the same now as when they were developed, much has changed in the tools and abilities of the instruments and methodologies.

Since then, multiple satellite missions equipped with advanced ocean colour instruments such as the Sea-viewing Wide Field-of-view Sensor (SeaWiFS) (McClain et al., 2004), the Moderate Resolution Imaging Spectroradiometer (MODIS) (Salomonson et al., 1989), the Medium Resolution Imaging Spectrometer (MERIS), the Visible Infrared Imaging Radiometer Suite (VIIRS), or the more recent, Ocean and Land Colour Instrument (OLCI), have been launched. Along with developments in the hardware and signal receiving side, there have been numerous developments in the application of these instruments. Similarly to how any spectral capturing device (such as a camera) has a spatial resolution, that is, the size of any given pixel within the image, there also exists a spectral resolution, that is, the the number, spacing, and width of wavelength bands recorded. The requirements for modern commercial devices such as a camera, is to satisfy the spectral resolution which best corresponds to our own spectral resolution (eyes). However, vastly different requirements need to be met when remotely sensing the constituents of the ocean. Additionally, spectral resolution, just like spatial resolution, requires further expense and equipment as more information is sought. Most ocean colour instruments used in the past decade are multi-spectral, measuring and recording radiance within multiple specific wavelength bands. These wavelength bands are selected with scrutiny and for specific purpose in the recording of the ocean and atmospheric optical signals. NASA's latest ocean-colour instrument on board the PACE (Plankton, Aerosol, Cloud, ocean Ecosystem) satellite is a hyper-spectral instrument, measuring the entire visible light and near-infrared spectrum in overlapping 5 nm bands. From here on, the word *band* is applied to mean the specific wavelength bands measured by ocean colour instruments on board earth observation satellites.

Many standard uses of single satellite sensor level 2 or level 3 products have been used within the Benguela for various applications. Examples using the SeaWiFS sensor at 4.5 km resolution include an analyis of short-term versus long term variability in chl-a concentrations (Demarcq et al., 2003) or the investigation of spatial and temporal variability in the Benguela ecosystem using a chl-a index (Demarcq et al., 2007). This chl-a index was based on a minimum threshold value (1 mg m^{-3}) that could be characterised as under the influence of coastal upwelling processes. This threshold was then applied to monthly averages to determine the size of the upwelling-influenced region and to analyse changes in temporal variability. Applications have also been used for ecological and biological research, such as using daily MODIS level 2, 1 km resolution observations as indicators of primary productivity in the Benguela (Grémillet et al., 2008). These daily observations were compared to three further trophic levels to identify match and mismatches between phytoplankton and their direct and indirect consumers. MODIS-Aqua monthly and seasonal climatology chl-a data, with a spatial resolution of 4.5 km has been used to investigate the relationship between phytoplankton communities and biogeochemical cycles through an adapted three-component model (Brewin et al., 2015; Lamont et al., 2018).

There have also been numerous studies within the Benguela which aimed to adapt or change satellite products to fit the regional requirements. Weeks (2004) produced a PhD thesis on using satellite remote

sensing to interrogate the upper surface level dynamics of the Benguela ecosystem. Since it was the first study of its time to interrogate the region using SeaWiFS high resolution spatial data (1 km), the authors found it required the modification of existing processing and bio-optical algorithms to better suit the study region. The paper builds upon an issue raised by Siegel et al. (2000), in which the assumption that water leaving radiance in the NIR is negligible (the black pixel assumption), breaks down in regions of high chl-a concentrations. Siegel et al. (2000)'s key takeaway from their analysis was that chl-a concentrations contribute to water leaving radiance in the NIR region through backscattering. If this is not accounted for, the atmospheric correction algorithm will assign it to atmospheric signal, hence an overestimating of aerosol reflectance (See section 2.3.2 for atmospheric correction formulation). The study suggests that regions of high chl-a concentrations will generate erroneous normalized water leaving reflectance values which in turn lead to erroneous chl-a estimates from the band ratios which depend on normalized water leaving reflectance.

Weeks (2004) worked closely with members of the SeaWiFS team to produce a new set of processing parameters as well as a new set of default flags for the processing chain. Following these corrections, they collected an in situ chl-a dataset consisting of 24 records for validation of the new parameters. Notably, despite making changes to the processing chain, there was no attempt to deviate from the standard in-water algorithm in use at the time, i.e. the OC4 O'Reilly and Werdell (2019).

Following the work done by Weeks (2004) a complete reprocessing of the SeaWiFS data was undertaken for the same time-series. Weeks et al. (2006) covers the results, as such, they too used a combination of high resolution (1 km) SST and chl-a data to study mesoscale upwelling features and consequential phytoplanktonic response. The SST data came from NOAA's AVHRR (Advanced Very High Resolution Radiometer) whilst the chl-a data came from SeaWiFS and covered a period from 1998-2003. Data was generated on a daily basis, but due to inherent limitations in the satellite orbits and swathe ranges, certain days had no associated data. As a result temporal interpolation was applied to all data using a 1/7, 5/7, 1/7 temporal weighted average (over the course of 3 day periods).

Whilst algorithm development for Case-2 waters had been a contentious issue in the mind of ocean optics experts since the fields emergence, Matthews et al. (2012) showed that the Benguela specifically, can be used as a targeted goal in the development of in-water algorithms. The main distinction is due to the Benguela's relatively unique optical properties when compared with the broad Case-1 and Case-2 definitions of water bodies, containing high phytoplanktonic constituents and concentrations but minimal sediment associated properties (Bernard et al., 2001).

Matthews et al. (2012) developed a maximum peak-height (MPH) algorithm working with 1 km spatial resolution MERIS bands in the red-NIR zone. The MPH algorithm is similar in philosophy to the flourescence line height(FLH) algorithm first developed for MERIS by Gower et al. (1999). The MPH algorithm searches for maximum peak in either the 681, 709 or 753 nm bands and uses whichever maximum in an equation along a baseline between 665 and 885 nm. The various maximum bands represent varying optical properties

which Matthews et al. (2012) argues can be associated with specific water bodies. The 681 nm band should be in maximum in low-medium biomass waters, where sun-induced chl-a fluorescence is optically dominant. The 709 nm band is in maximum in high biomass waters where chl-a absorption may reduce the reflection observed in the 681 band and increased particulate backscattering drives the reflectance to a near 700 nm peak. The product was developed by applying the algorithm to Rayleigh-corrected reflectances.

Other approaches have been taken to adjust and reform existing algorithms to better suit the Benguela, Smith et al. (2018) built upon some of the methods and data from the bio-optical models developed in Lain et al. (2014) to establish an optimized chl-a switching algorithm based on the ratio between the MERIS/OLCI bands 708 nm and 665 nm. Lain et al. (2014)'s bio-optical model related a Benguela-typical phytoplankton assemblage of dinoflagellates and the associated IOPs to the expected AOPs generated. The study confirmed the appropriate emphasis on analysing the red-NIR region of spectra in regions of high chl-a, but more importantly, confirmed the use of this methodology within a range of IOPs explicitly expected within the Benguela region. The study found that a chl-a concentration of 15 mg m^{-3} represented the zone where "the red features of high biomass reflectance spectra start to dominate". The 708 and 665 nm bands represent wavelengths that change dramatically with increasing chl-a concentrations. At around 700 nm, the phytoplanktonic backscatter builds a reflectance peak, whilst at 675 nm, chl-a absorption causes a reflectance trough.

Even with global extent covered by orbiting satellites, gaps are common and frequent due to factors such as cloud cover, smoke, dust/ash plumes or other failure inducing mechanisms like glint. Hence the ability to produce a global scale resolution on a short temporal period (daily for example) can be improved significantly by combining multiple overlapping satellites. Since earth observation satellites rely on carefully and accurately calibrated equipment, each earth observation satellite is built with a specific mission time and objective (Fig 2.4), after which, they are potentially unviable for use in accurate data collection.

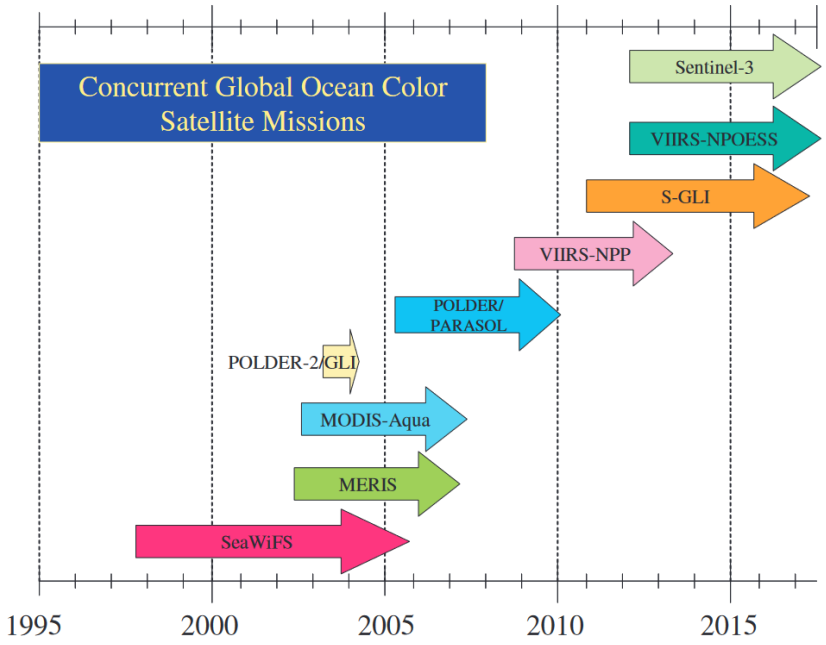

Figure 2.4: Mission periods for global earth observation satellites, sourced from IOCCG (2007)

The overlapping of mission periods presents an opportunity to form a merged product, consisting of data collected from multiple individual earth observation satellites. This was recognised even in the very first years of overlapping global missions between SeaWiFS and MODIS, as was shown in Gregg and Woodward (1998). The baseline goals for a merged data product are: 1) daily global coverage, 2) high accuracy and consistency, and 3) high spatial resolution. In theory, the ability to merge multiple concurrent sources can improve both stochastic errors (through an increased quantity of measurements n) and systematic errors (through instrument cross calibration). There are many application benefits to merged products as well: climate models benefit from the enhanced statistical consistency and global coverage, global biogeochemical cycles will be able to be interpreted with better context, and the broader scientific and public communities can benefit from an all-in-one merged data product (IOCCG, 2007).

ESA has developed two concurrent global and multi-satellite chl-a datasets available for use through the Copernicus Marine Service (CMEMS), the Copernicus GlobColour and OC-CCI datasets. A detailed and technical description of these products is given in Chapter 3.1.2. The production philosophy between these two products is fundamentally different. GlobColour is produced on a daily basis with Near Real Time (NRT) production and then recalibrated into a consistent Multi-Year (MY) product at a later stage. This allows quick and relevant daily observations but with potential inaccuracy and changes when the yearly recalibration takes place. OC-CCI is produced intentionally as a GCOS' ECV product and hence prioritises stable long-term consistency climate science applications.

The use of merged satellite products has also been covered within the Benguela region, van Oostende et al. (2023) for example, after applying a novel correction to account for claims of temporal inconsistency in the OC-CCI dataset, used it to diagnose global ocean colour trends in biogeochemical provinces, including the

Benguela

Outside of the Benguela, merged satellite products have been compared to each other and to other single sensor products at both regional and global extents. Regionally, studies have compared the performance of multi-satellite products to single sensor products in areas such as the Northern Persian Gulf (Moradi, 2021, 2022) and British Columbia coastal waters (Pramlall et al., 2023). Additionally there have been many studies comparing performance at global scales such as Couto et al. (2016) and Pardo et al. (2024).

There is a varied and extensive historical record of ocean colour work within the Benguela region, with applications to many adjacent scientific fields. Additionally, the validation and performance of merged satellite products against in situ results, single sensor products, and other merged products has been performed at both the global and coastal level. However the comparison and validation of merged satellite products remains largely undone within the Benguela. Historical studies have proven the potential difficulty and attention required to accurately estimate chl-a within this region, hence a dedicated study analysing the performance of the two most popular merged products and their ability to estimate chl-a within the Southern Benguela region is an obvious objective for the local oceanographic and remote sensing community.

Chapter 3

Data and Methods

3.1 Data

3.1.1 Study region and in situ data

The region of study in this project is spatially represented from 17-20 degrees East and 31-35 degrees South as shown in Figure 3.1, covering parts of the west coast of South Africa, past the Cape of good hope, and extending to Cape Agulhas in the south.

Collation of in situ chl-a data was assembled from two sources. The first was an already curated dataset provided by the Council for Scientific and Industrial Research (CSIR), which contained Latitude, Longitude, Date/time and chl-a concentration data collected from various sources by the South African Department of Forestry, Fisheries and the Environment (DFFE), the CSIR, The University of Cape Town (UCT) and the SEAHAB project (Sensor-agnostic Estimation of Harmful Algal Blooms) Smith (2025). This dataset spanned from 2002-2012 and 2017-2023.

The second source of in situ data was the PANGEA website (Felden et al., 2023). PANGEA is a data collection and publishing website designed for Earth and Environmental Science. Data was downloaded directly from the website. A total of 4 independent datasets were used from PANGEA. These included: 1) the OC-CCI's collated dataset of chl-a used for their own model validation (Valente et al., 2022); 2) NASA's bio-Optical Marine Algorithm Data set (NOMAD), an in situ collated dataset used for NASA's ocean colour algorithm development and satellite product validation (Werdell and Bailey, 2005); 3) the in situ dataset used by the CoastColour project (Nechad et al., 2015), and 4) a collection of chl-a data taken from underway cruise sampling across the Agulhas bank (de Villiers, 2017).

The PANGEA data required data exploration and cleaning which was done using the coding language Python and the Python package *pandas* (McKinney et al., 2010). The data was subset to fit the spatial extent of the study region, and chl-a, Longitude, Latitude and Date/Time variables were standardized. The five datasets were then collated into a single database with columns, chl-a, latitude, longitude and

Date/Time for use in analysis.

The in situ data was cleaned for erroneous points by removing any data points that had negative chl-a values. Since the collated in situ data contained multiple datasets which themselves were collations, checking for duplicated points was required. Any points which contained the same latitude, longitude and Date/Time were considered duplicates and only the first instance kept. Additionally any points which contained the same latitude, longitude and chl-a were additionally considered duplicated and only the first instance kept. After duplication checks, the NOMAD data set was completely excluded (Since the OC-CCI dataset had incorporated NOMAD, all the data points were duplicated). The final collated dataset includes 4 sources and covers a wide range of conditions and locations along the study region (Fig 3.1) (Table 3.1).

Table 3.1: In situ chl-a data sets used in this study.

Dataset	n	Method	Reference
CSIR	491	Fluorometric analysis	Smith (2025)
OC-CCI	142	High Performance Liquid Chromatography (HPLC), Fluorometric analysis	Valente et al. (2022)
CoastColour	95	Fluorometric analysis	Nechad et al. (2015)
deVilliers	106	Not applicable	de Villiers (2017)

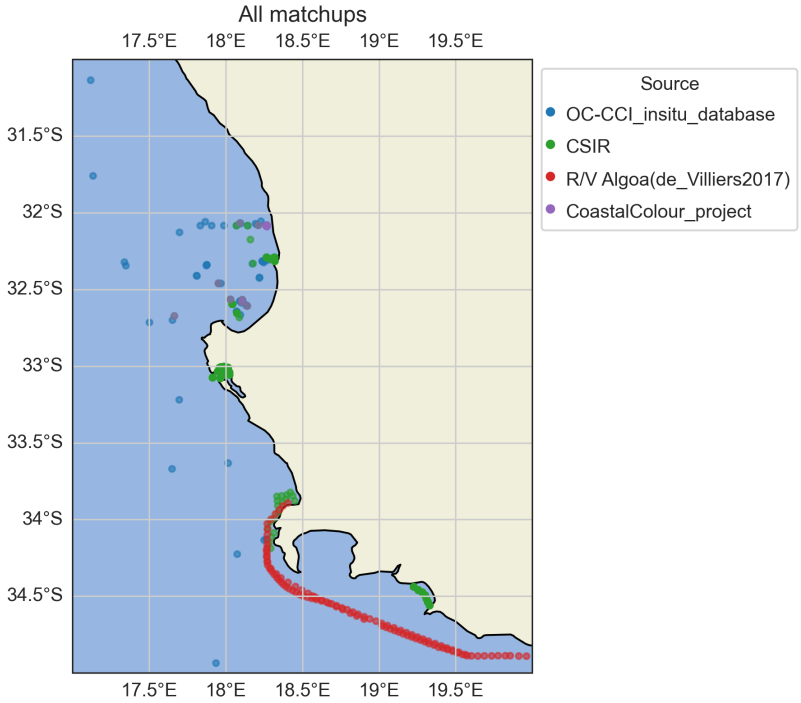

Figure 3.1: Location and source of in situ chl-a data (N = 834)

3.1.2 Satellite data

GlobColour

The GlobColour merged chl-a data product is a global, multi satellite and long-term time series product provided by ACRI-ST for the Copernicus Marine Environmental Monitoring Service (CMEMS). The GlobColour processing unit first begun development in 2005, with the goal of providing a continuous data set of merged Level-3 ocean colour products.

Since its 2018 iteration, the GlobColour product has used a combination of three in-water algorithms. The Chlorophyll Index (CI) (Hu et al., 2012) for oligotrophic conditions, a sensor-dependent OCx algorithm (O'Reilly and Werdell, 2019) for mesotrophic conditions, and the OC5 algorithm (Gohin et al., 2002) for complex and eutrophic conditions (Garnesson et al., 2019).

The GlobColour product involves merging level 2-input data from SeaWiFS (1997–2010), MERIS (2002–2012), MODIS Aqua (2002–present), VIIRS-NPP (2012–present), OLCI-S3A (2016–present), VIIRS JPSS-1 (2017-present) and OLCI-S3B (2019-present) sensors, running a time series from 1997-present. When these data products overlap spatially and temporally, there are many advantages to merging the products, such as reducing sensor bias and reducing stochastic error by increasing sample sizes.

The GlobColour merging process occurs in two stages. An initial mono-sensor chl-a concentration is computed for each sensor using it's characteristic bands and resolutions. These mono-sensors are then re-sampled and merged. The processing unit also employs it's own flagging strategy, deviating from the standard flags provided by space agencies to their level 2 products. These deviations include a lower level of flagging to improve spatial and temporal coverage and adjusted parameter thresholds for sensor flags, inherited from the OC5 algorithm (Garnesson et al., 2019).

Level-4 GlobColour data involves either a temporal averaging method or an interpolation procedure to correct and fill in missing data. This level of product is often known as a 'gap-free' or 'cloud-free' product

Level-4 processed GlobColour data, with a daily temporal resolution and 4 km spatial resolution was downloaded for this study. Both global datasets were downloaded with the spatial extent matching the study region (17-20 degrees East and 31-34 degrees South), and temporal extent matching the in situ range (1997-2022). The data were accessed from the Copernicus Marine data store `https://doi.org/10.48670/moi-00281` on date 2024/10/10 , with variables 'Mass concentration of chl-a in sea water' and 'Status flags'.

OC-CCI

The OC-CCI is the Ocean Colour chapter of the ESA Climate Change Initiative (CCI) programme, established to generate a set of validated and error-characterised Essential Climate Variables (ECVs). The OC

chapter began development in 2010 and has since revolved around a number of research phases. The current iteration is the OC-CCI+ phase starting in 2019.

The OC-CCI uses level-1 and level-2 input data from the SeaWiFS (1997–2010), MODIS (2002–2019), VIIRS (2012–2019), OLCI-S3A (2016–present), and OLCI-S3B (2019-present) sensors whilst adapting them to a baseline sensor, MERIS (2002–2012). The processing chain involves using the POLYMER algorithm (Steinmetz et al., 2011) for level-1 MERIS, MODIS, VIIRS and OLCI data and the NASA L2gen algorithm for level-1 SeaWiFS data, to produce level-2 products (Jackson et al., 2022).

All non-baseline sensors were band shifted to match the MERIS bands of 412, 443, 490, 510, 560 and 665 nm using a quasi-analytical algorithm (Lee et al., 2009) to determine the IOPs and then a subsequent high resolution spectral model to compute them back into the relavent R_{rs} bands. After correcting for sensor biases, the individual sensor data (still level-2 reflectance) are merged using a simple average. This is notably different from the GlobColour processing unit, which only merges the products once they have been converted to chl-a by the individual sensors.

The OC-CCI uses a water class membership system following Moore et al. (2009), but adapted to include 14 water classes (Jackson et al., 2022).These water class memberships are used to allocate the weighting of a series of blended in-water algorithms. These include the OCI (Hu et al., 2012), OCI2, OC2 and OCx algorithms O'Reilly and Werdell (2019).

The flagging protocol of OC-CCI uses generic flagging for level-2 input products (SeaWiFS) and a generic pixel classification algorithm (Idepix) when data are processed by POLYMER.

Level-3 processed OC-CCI data, with a daily temporal resolution and a spatial resolution of 4 km, were downloaded for this study. Both global datasets were downloaded with the spatial extent matching the study region (17-20 degrees East and 31-34 degrees South), and temporal extent matching the in situ range (1997-2022). The data were accessed from the Copernicus Marine data store `https://doi.org/10.48670/moi-00282` on date 2024/09/23, with variables 'Mass concentration of chl-a in sea water'.

Sentinel-3 OLCI product

The third satellite dataset was obtained directly from the CSIR (Smith, 2024). This product featured daily 300 m resolution data from the Sentinel-3A and Sentinel-3B Ocean and Land Colour Instrument (OLCI). The chl-a estimation used in this product comes from an optimized algorithm developed specifically for use in the Benguela region by using specific thresholds of the 709/665 nm band ratio to define where different chl-a algorithms should be applied, using OCI algorithm (O'Reilly and Werdell, 2019) for low ratios (more oligotrophic conditions), the G2B algorithm (Gitelson et al., 2010) for higher ratios (more eutrophic conditions) and a blended product in-between (Smith et al., 2018).

The total range and comparison of in-water algorithms and sensors used in all three products can be seen in Table 3.2

Table 3.2: Multi and mono-sensor products used in this study, and their varying features

Product	Level	Time period	In water Algorithms	Sensors
OC-CCI	Lvl-3	1997-2024	OCI, OCI2, OC2, OCx blend	SeaWiFS, MODIS, MERIS, VIIRS, OLCI-3A, OLCI-3B
GlobColour	Lvl-4	1997-2024	OCI,OC5	SeaWiFS, MODIS, MERIS, VIIRS, OLCI-3A, OLCI-3B
Sentinel	Lvl-3	2016-2024	OCI,G2B	OLCI-3A, OLCI-3B

3.2 Analysis

3.2.1 Extraction and Match-up

In order to perform validation on the various satellite products, the most relevant pixel or *match-up* for each in situ data point was identified from each product respectively. This was done using Xarray (Hoyer and Hamman, 2017) and Pandas packages within Python in a two step process: 1) the appropriate daily slice was determined for each data point, and 2) the closest pixel spatially to the data point was determined within that daily product. Once the pixel had been identified, its chl-a value was determined.

A 3x3 megapixel centered over the pixel closest to the in situ station was built for consistency sake. If the 3x3 megapixel contained 5 or more valid results (not NAN's), the mean chl-a, standard deviation (Std) and number of valid pixels within the megapixel were extracted. This mean value was calculated as a simple average of all valid pixels within the 3x3 box. This process was repeated iteratively for each in situ data point and for each satellite product. Since the Sentinel product only begun in 2016, its extraction and match-up process only used in situ data from 2016 onwards. Once the 3x3 megapixel match-up had been extracted, the difference between it's calculated mean (modelled response) and the in situ value (observed response) was determined. This difference was additionally recorded in base 10 for use in statistical performance metrics (Log-Diff). (Fig 3.2)

A series of datasets corresponding to different validation steps were built throughout the match-up process as per Bailey and Werdell (2006) (Fig 3.2). Any 3x3 megapixels that contained pixels already used in the analysis were removed to avoid duplicated match-ups. A coefficient of variance (CV) was calculated (Standard deviation/Mean), and where CV exceeded 0.2, the results were excluded from analysis. Additionally, the match-ups for the GlobColour product were built after removing all data points that contained the interpolation flag (hence removing any interpolated data points).

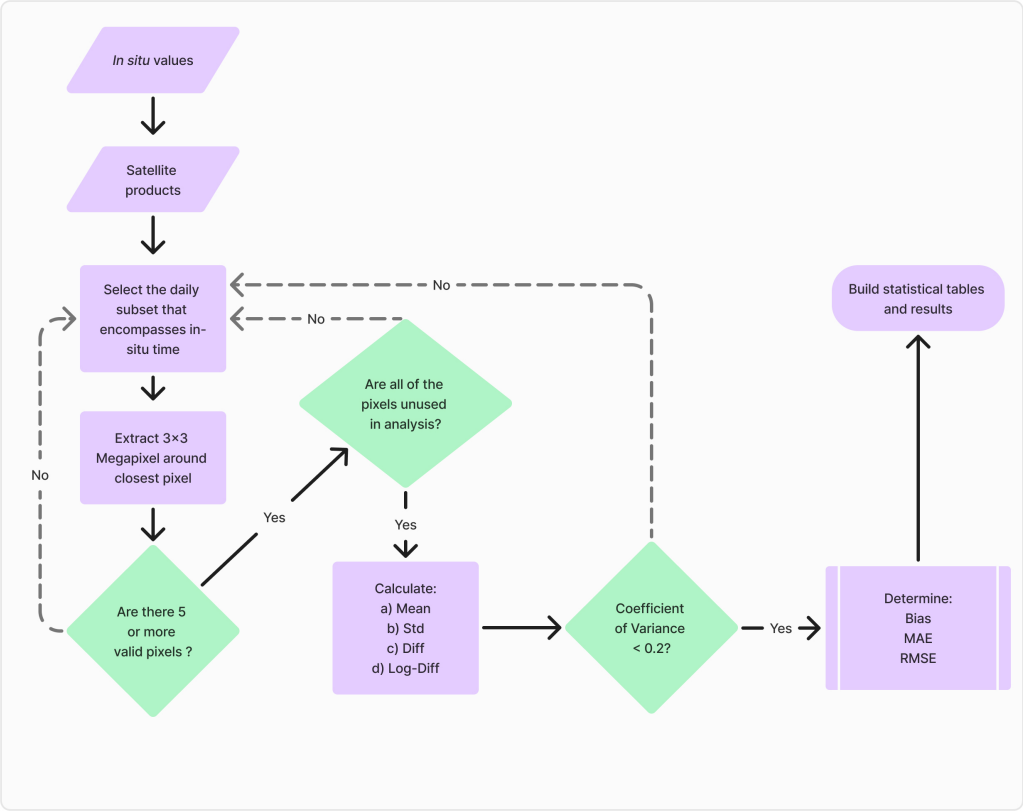

Figure 3.2: Flowchart of the procedures applied to extract match-up values.

3.2.2 Trophic classification

In order to further interrogate the performance of the datasets. The in situ points and associated match-ups were split into oligotrophic (chl-a < 1 mg m^{-3}), mesotrophic ($1 <$ chl-a < 15 mg m^{-3}) and eutrophic (chl-a > 15 mg m^{-3}) conditions. This allows the comparison of performance whilst isolating the effect of biomass.

3.2.3 OC-CCI subset

A second subset of results was built by removing any match-ups that were found to be invalid for the OC-CCI product from both other products. These invalids are match-up pixels which the OC-CCI product does not contain a chl-a value for, either due to a failure of the algorithm, a flagging protocol, or a gap in data (cloud cover or satellite swath extent). The objective of this was to indicate the direct role of processing choices in the development of ocean colour products, and the degree to which these can affect the ability and performance of said products. This set of results here-on is named the OC-CCI subset.

3.2.4 Statistical performance metrics

The statistical procedure in this study follows those procedures laid out and motivated by Seegers et al. (2018). The ultimate objective of performance metrics is to determine the extent of systematic error (in the form of bias), stochastic error (in the form of variability) and a combination of the two (in the form of accuracy) found within the modelled response. As such, performance metrics rely on some 'truth' value which takes the form of the observed variable, and a modelled value. Whilst these truth values (in situ chl-a in this case) are never actual truths, they represent the best possible baseline of said variable we are able to obtain.

Importantly, this study does not pretend to present the performance of in-water algorithms in isolation. There are many processes and choices in the generation of chl-a values that can cause the result to vary from product to product (see 2.3). Due to the intrinsically different methods in which the OC-CCI and GlobColour products are built, as well as their differences to a mono-sensor product such as the one used in this study, the effects of in-water algorithms cannot be isolated from the performance of said products. Instead the results generated represent the differences that arise from all processing choices and methods used in the product development.

Error metrics

The first performance metric used in this study is bias. Bias is a simple and easy to interpret metric that measures the models systematic error i.e it provides us the ability to tell whether a model is overestimating or underestimating its result in comparison to observed values. Bias is represented as follows:

$$\text{Bias} = 10\text{^}(\frac{\sum_{i=1}^{n} \log_{10}(M_i) - \log_{10}(O_i)}{n}) \tag{3.1}$$

where M, O and n represent the Modelled value, Observed value and number of samples respectively.

The second metric used in this study is Mean Absolute Error (MAE). Typical statistical performance metrics used in ocean colour studies include root mean square error (RMSE), coefficient of determination (r^2) or the regression slope (Weeks, 2004). In comparison to MAE , RMSE is far more sensitive to outliers due to it's squaring of errors. This poses a problem for validation datasets that don't follow a Gaussian distribution of errors. For this reason Seegers et al. (2018) recommends the use of MAE as an accuracy metric. Measures of RMSE have been calculated and included in this study for the sake of inter comparison with other studies of a similar nature. MAE and RMSE values reported in this study are taken from the formulas that follow:

$$\text{MAE} = 10\text{^}(\frac{\sum_{i=1}^{n} |\log_{10}(M_i) - \log_{10}(O_i)|}{n}) \tag{3.2}$$

$$\text{RMSE} = \sqrt{\frac{\sum_{i=1}^{n} (M_i - O_i)^2}{n}} \tag{3.3}$$

Both Bias and MAE metrics used in this study are log-transformed. This is not uncommon for a marine geophysical variable, as the data response often covers multiple orders of magnitude (especially for regions of high variability such at the Southern Benguela). Since chl-a estimates carry uncertainties which scale proportionally to its value, the error terms are better represented by a multiplicative scale. The statistics are calculated within log_{10} space and then converted back out again for sake of interpretation. As such, a Bias of 0.8 indicates the model response is on average 0.8x the value of the observed variable. An MAE of 2 indicates a measurement error of 100%.

3.2.5 Application Case Study

A targeted area of longitude 17.5 to 19 degrees East and latitude 31.5 to 33.5 degrees South was chosen to test the application of all three products and their ability to capture a variety of conditions. This area marks the greater St. Helena bay region, in which a mixture of upwelling and hydrographic features such as water retention often lead to high biomass blooms during the summer months. This case study was applied via two methods: a) comparison of visual chl-a plots for each product during a high biomass bloom event that occurred in the later portion of February 2022, and b) comparison of the daily 95th percentile chl-a values in a time series of the area, over the course of a year for each product. 2022 was selected as the case year due to it's well documented hypoxic events, resulting in large scale rock lobster walk outs (Mbelengwa, 2023). Monthly averages of mean chl-a were also graphed for the same year, to assess the effects of spatio-temporal averaging on seasonal signals. Testing a year with known high biomass blooms and subsequent effects allows us to best test a variety of conditions. The visual method allows easy comparison of spatial heterogeneity whilst the time-series method allows for comparison of temporal heterogeneity.

Chapter 4

Results

4.1 Results for all match-ups

Model to observed (satellite to in situ) match-ups were produced for each product. Scatter plots of the *Log10* modelled to observed chl-a values were plotted (Fig 4.1). OC-CCI showed a pattern of underestimation at high in situ values and overestimation at low in situ values. GlobColour showed a similar pattern with many large underestimations at high in situ values and overestimations at low in situ value. In contrast, the Sentinel-3 product showed a slight but consistent overestimation at almost all values of chl-a concentration, along with a smaller spread of data and a slope far closer to 1 (Fig 4.1).

These results are supported by their probability density functions, where the tail of the distribution on either side represent the more extreme outlying modelled responses (Fig 4.2). The x-axis of these graphs represent the ratio of modelled and observed chl-a concentrations. A high ratio shows the model estimated a higher chl-a value than observed (overestimation) whilst a low ratio shows the model estimated a lower chl-a value than observed (underestimation). The density (y-axis) shows the probability density of each product to produce said ratio. The Sentinel product's density function shows a distinctly non-Gaussian distribution, with a primary peak close to 0 and broad right side tail, only tapering off close to 0.5, indicating overestimation (Fig 4.2). The broader right side tail could be representative of a closely grouped set of low chl-a match-ups, all of which the Sentinel product overestimates (Fig 4.1). Both global products show broader left side tails, with the OC-CCI's extending the furthest, indicating a higher possibility of underestimating chl-a compared to the Sentinel product.

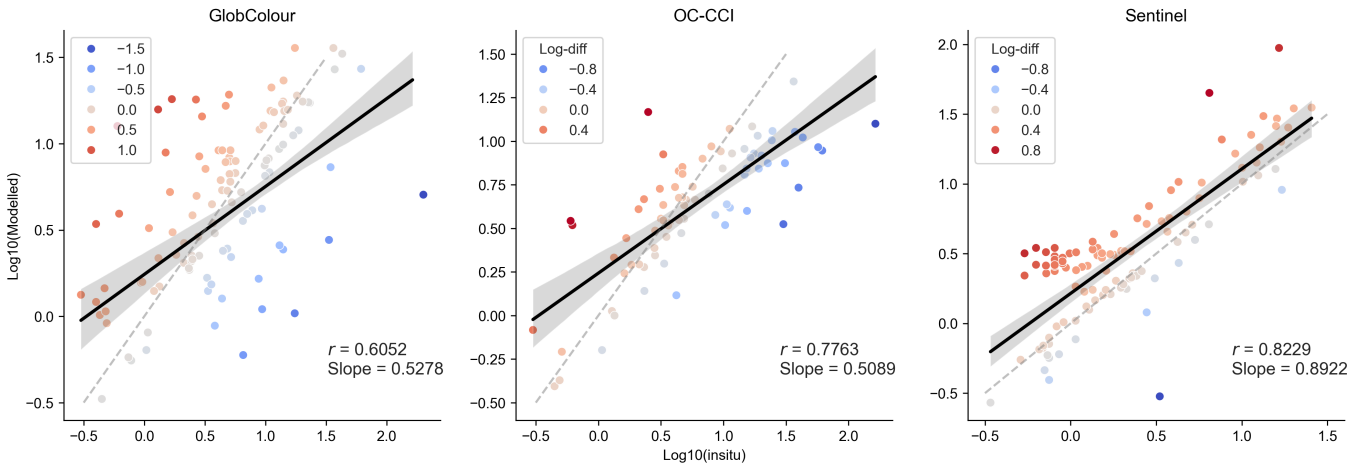

Figure 4.1: Scatter plots showing the *log10* modelled and in situ chl-a values for each match-up. Points are coloured by their *log10* difference. The solid line indicates the linear regression of the points with the shaded area representing the confidence interval. The dotted line represents a 1:1 relationship. N = 79, 112 and 114 for OC-CCI, GlobColour and Sentinel respectively.

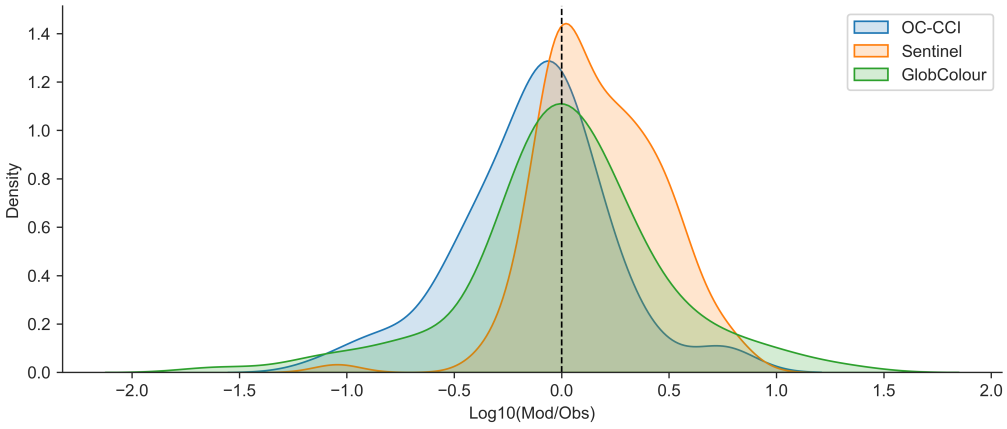

Figure 4.2: Kernel Density Estimate (KDE) graph for all three models, The probability density function is given of the *log10* ratio between Modelled and Observed chl-a.

Quantitatively, Sentinel and GlobColour found 114 and 112 match-ups respectively, whilst OC-CCI had considerably fewer match-ups (79). OC-CCI was found to have a Bias of 0.74, indicating on average, an underestimation of the observed chl-a. GlobColour showed a Bias of 1.04 whilst Sentinel showed a bias of 1.51 indicating on average, an overestimation of observed chl-a. The Sentinel-3 product showed the lowest MAE (Mean Absolute Error) of 1.77 followed by OC-CCI (1.88) and GlobColour (2.07) (Table 4.1)

Table 4.1: The number of valid match-ups (n), bias, MAE, RMSE, and metric statistics for all datasets

Dataset	n	Min	Median	Mean	Max	Bias	MAE	RMSE
OC-CCI	79	0.39	4.62	5.58	22.01	0.74	1.88	0.37
GlobColour	112	0.33	5.03	7.76	35.85	1.04	2.07	0.45
Sentinel	114	0.27	2.82	6.64	94.15	1.51	1.77	0.33

When the match-ups are categorised into oligotrophic (chl-a $<$ 1 mg m^{-3}), mesotrophic (1 $<$ chl-a $<$ 15 mg m^{-3}) and eutrophic (chl-a $>$ 15 mg m^{-3}) conditions, there are clear patterns in product performance. All three products show a large overestimation of oligotrophic conditions (Table 4.2), as well as higher MAE scores in comparison to mesotrophic conditions (Table 4.3). It is critical to mention that both OC-CCI and GlobColour found <30 valid match-ups in oligotrophic conditions. This can be partly explained by the number of oligotrophic in situ data points available (114 out of 832 total in situ points). The Sentinel product contains >30 match-ups for oligotrophic conditions, yet still shows markedly different MAE when compared to mesotrophic conditions (Table 4.3). All three products show higher MAE's in eutrophic conditions compared to mesotrophic conditions, with GlobColour and OC-CCI both producing low biases indicating underestimation whilst the Sentinel product maintained a high bias indicating overestimation (Table 4.4). In comparison with other water types, OC-CCI showed the poorest performance in eutrophic conditions, while both Sentinel and GlobColour showed the poorest performance under oligotrophic conditions.

Table 4.2: The number of valid match-ups (n), bias and MAE for match-ups with chl-a $<$ 1 mg m^{-3}

Oligotrophic	n	Bias	MAE	RMSE
OC-CCI	6	2.07	2.27	0.47
GlobColour	14	2.56	2.91	0.58
Sentinel	33	1.98	2.27	0.44

Table 4.3: The number of valid match-ups (n), bias and MAE for match-ups with 1 $<$ chl-a $<$ 15 mg m^{-3}

Mesotrophic	n	Bias	MAE	RMSE
OC-CCI	53	0.93	1.48	0.23
GlobColour	82	1.05	1.9	0.38
Sentinel	72	1.34	1.59	0.27

Table 4.4: The number of valid match-ups (n), bias and MAE for match-ups with chl-a $>$ 15 mg m^{-3}

Eutrophic	n	Bias	MAE	RMSE
OC-CCI	20	0.30	3.35	0.59
GlobColour	16	0.45	2.45	0.61
Sentinel	9	1.45	1.75	0.31

4.2 OC-CCI subset

Analysis of dataset statistics showed the OC-CCI subset had both a higher mean and median chl-a concentration (Table 4.5). Points were arranged in ascending chl-a concentration to determine the minimum (min), median, first quartile (Q1), third quartile (Q3) and maximum (max) of both in situ datasets. Spatial comparison of match-ups between all results (N = 252) and the OC-CCI subset (N = 158) show a large number of discrepancies in Saldanha bay, along Cape Towns Atlantic coast, and along a tract of offshore samples (34-35 degrees South and 18.25-19 degrees East). Almost all points removed featured within the lower end of chl-a concentrations (Fig 4.3), this can be quantitatively seen in the statistical differences between the two sets of match-ups (Table 4.5).

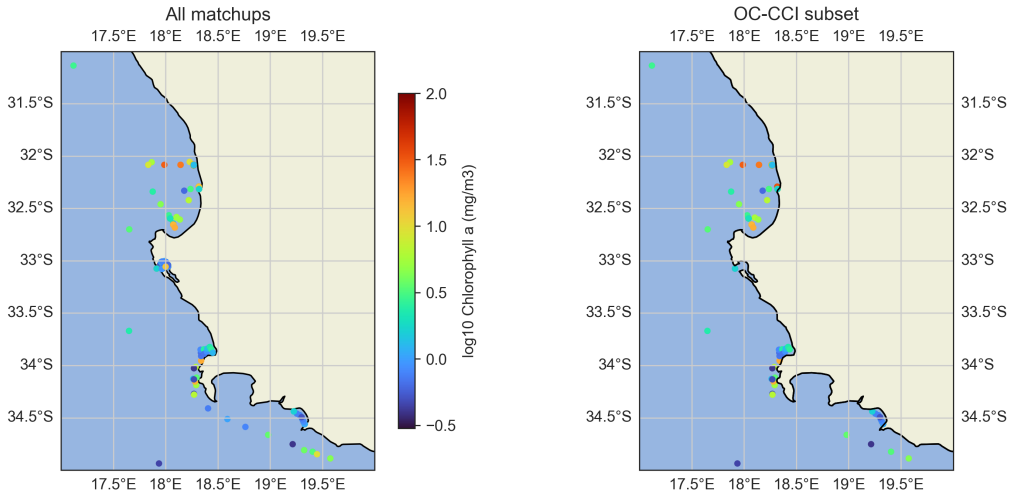

Figure 4.3: Locations of in situ data points used for all match-ups (N=252) and the OC-CCI subset (N=158), those points which did not make it through quality control are not shown. Points are coloured by logged in situ chl-a concentration.

Table 4.5: Various statistics for both the original and OC-CCI subset of in situ data.

	n	Min	Q1	Mean	Median	Q3	Max
All in situ match-up points	252	0.3	1.34	8.33	3.34	9.87	201
OC-CCI subset	158	0.3	2.45	10.18	4.69	11.43	163.7

GlobColour is reduced to 75 match-ups after excluding OC-CCI invalid match-ups, whilst the Sentinel product is reduced to 57 match-ups (Table 4.6). GlobColour shows a slightly higher bias compared to all match-ups, but almost no change in MAE. The Sentinel product shows both a lower bias and a markedly lower MAE (Table 4.6) compared to all match-ups. These changes in both precision and accuracy can be seen in the Sentinel product's probability density function, where the broad band of overestimations has been removed almost completely (Fig 4.5), as well as it's scatter plot, where a grouping of overestimations around x=0 evident in Fig 4.1 have been filtered out (Fig 4.4).

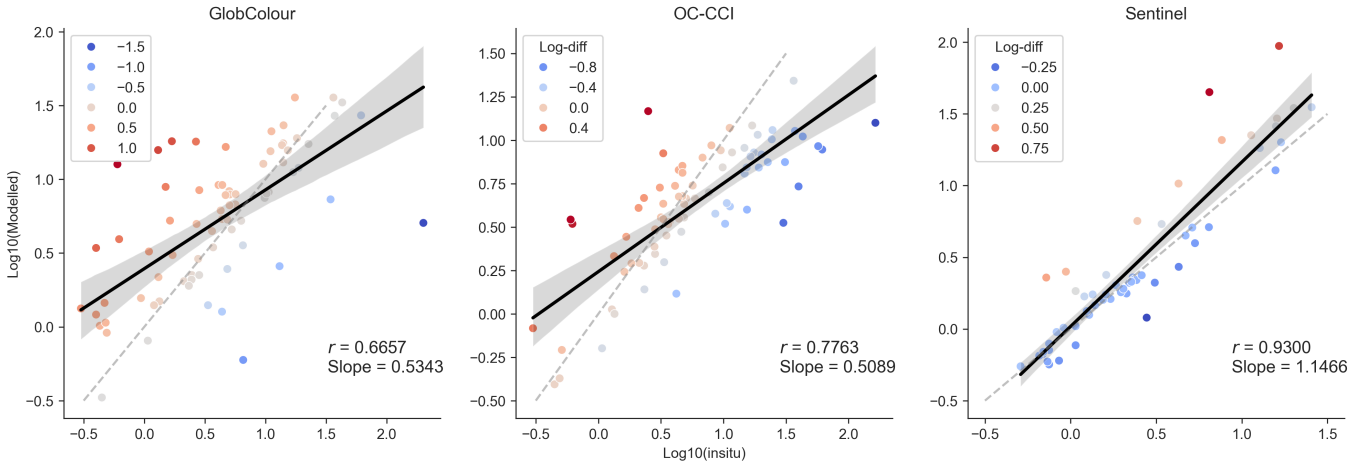

Figure 4.4: Scatterplots showing the *log10* modelled and in situ chl-a values for each match-up of the OC-CCI subset. Points are coloured by their *log10* difference. The solid line indicates the linear regression of the points with the shaded area representing the confidence interval. The dotted line represents a 1:1 relationship. N = 79, 75 and 57 for OC-CCI, GlobColour and Sentinel respectively.

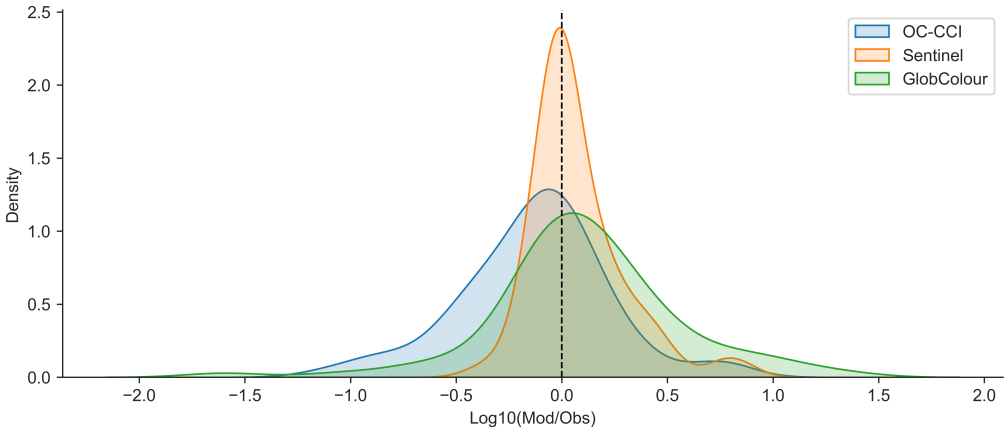

Figure 4.5: Kernel Density Estimate (KDE) graph for all three models of the OC-CCI subset.

Table 4.6: The number of valid match-ups (n), bias and MAE for all match-ups within the OC-CCI subset

OC-CCI subset	n	Bias	MAE
OC-CCI	79	0.74	1.88
GlobColour	75	1.28	2.06
Sentinel	57	1.19	1.40

4.3 Case study application

Visual plots of chl-a (Fig 4.6) clearly show differing abilities in pixel retrieval. The GlobColour product produces the least flagged pixels, minimising flags such as the cloud cover clearly visible in both other products on the 20th and 24th. The GlobColour product also appears to show some data inside the small coastal embayment of Saldanha Bay (near 33 degrees South and 18 degrees East). The OC-CCI product has

the same spatial resolution but appears to consistently flag more pixels along and close to the coast. There are also noticeable differences in chl-a values in certain regions and days when compared to GlobColour, such as Saldanha bay on the 18th and St Helena bay on the 20th. The Sentinel-3's 300 m resolution allows for a larger total pixel count for the same area. Additionally the Sentinel-3 product captures far higher maximum chl-a values, reaching maximums of 300 mg m^{-3}. This tendency for a higher maximum peak by Sentinel-3 can be seen again in the 95th percentile time-series plot (Fig 4.7). Despite each point being a 95th percentile of all pixels for that day, there are clearly peak bloom values influencing the Sentinel-3 averages, resulting in values 3x and sometimes 4x those of the global products. Between the two global products, OC-CCI seems to estimate consistently lower chl-a values across all seasons when compared to GlobColour. Monthly data shows that all three products estimate similar seasonal patterns in chl-a values, but with disagreements on the magnitude of chl-a concentrations (Fig 4.8).

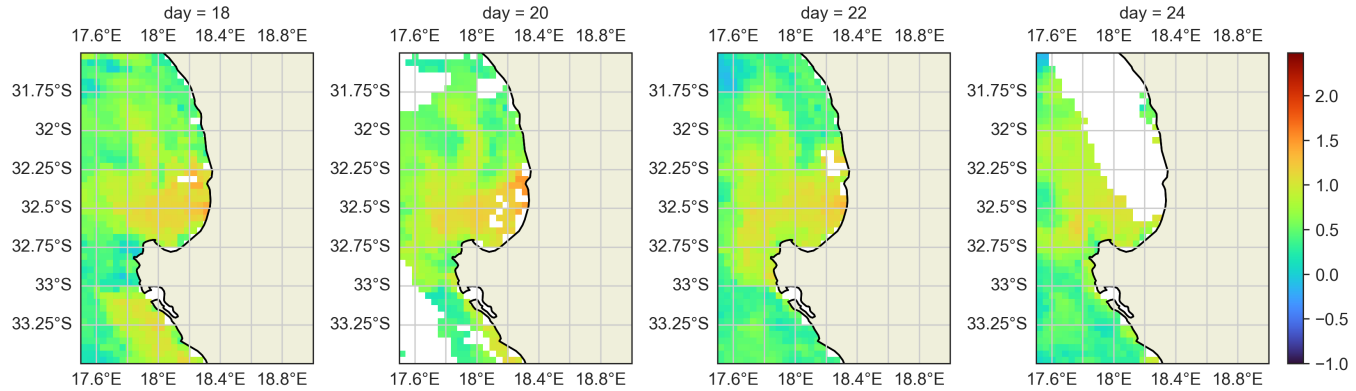

(a) OC-CCI

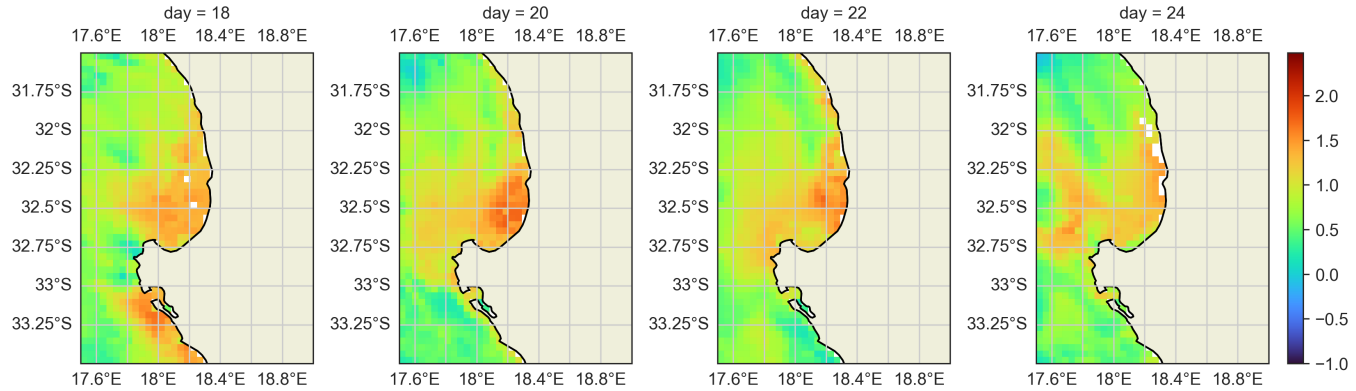

(b) GlobColour

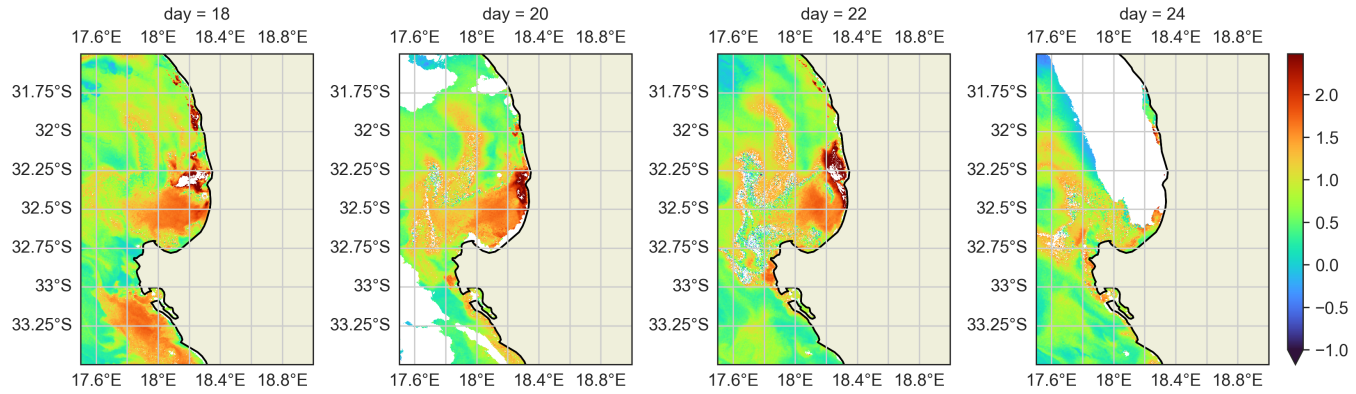

(c) Sentinel

Figure 4.6: Log10 chl-a concentration in the St Helena Bay area provided by the OC-CCI (top), GlobColour (middle) and Sentinel (bottom) products on the 18th, 20th, 22nd and 24th day of February 2022

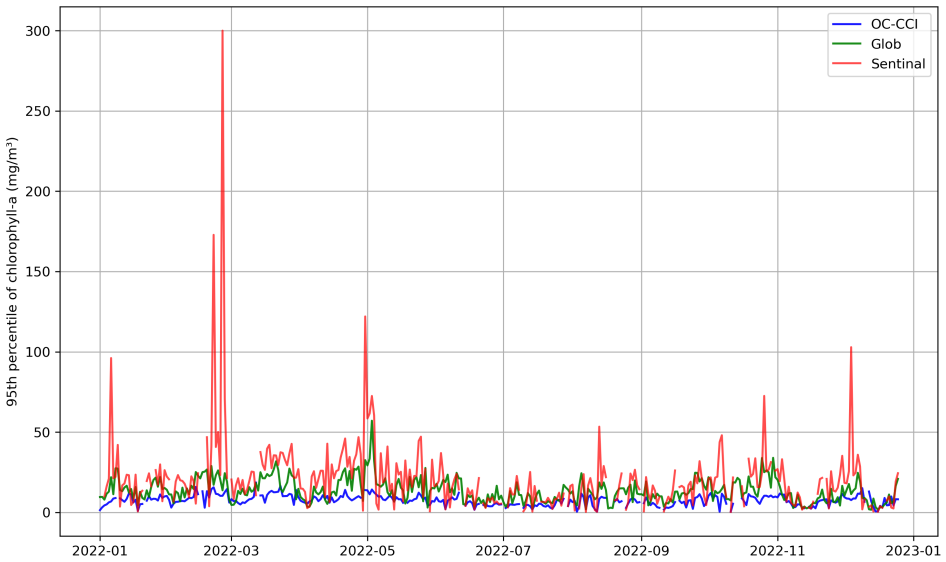

Figure 4.7: 95th percentile daily chl-a values for all three products (2022)

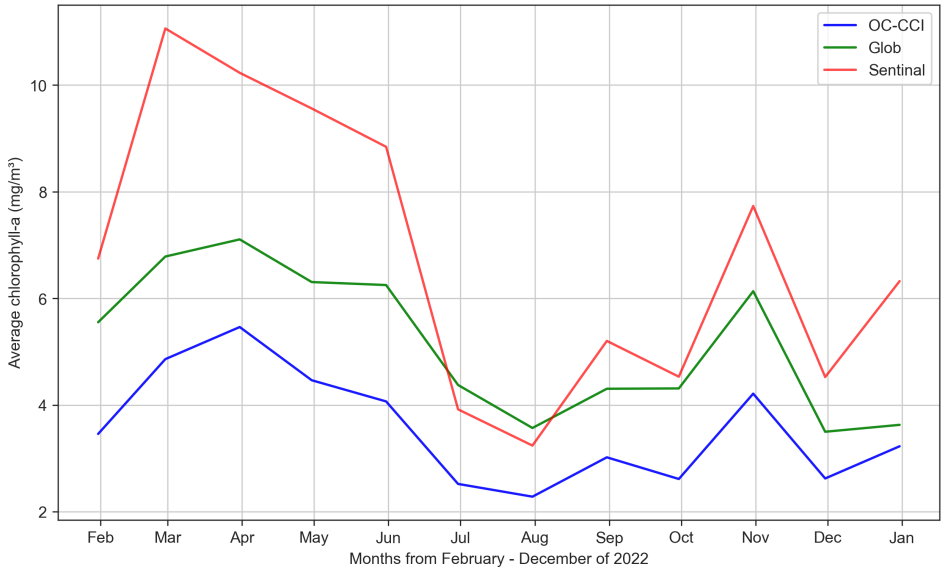

Figure 4.8: Mean monthly chl-a values for all three products (2022)

Chapter 5

Discussion

5.1 Scope and limitations

The scope of this project is a methodological one, aimed at comparing the methods and performance of multiple satellite products within the study region. The goal of this project is not to obtain definitive chl-a results in the region, as this would call for a more in-depth application and potential development of a chl-a product.

The ability to provide satellite validation is unavoidably dependent on the in situ database used. Chl-a validation requires specific requirements of its in situ data, which ideally would include: 1) spatial spread to the extend that it covers multiple satellite resolution pixels and hence multiple match-ups; 2) chl-a concentrations measured within the top 5 metres of the surface ocean; 3) temporally spread to allow for multiple daily match-ups; and 4) accurate longitude and latitude data. Additionally, AOPs measured in situ alongside the chl-a measurements are often asked for in the validation stages of performance studies (Bailey and Werdell, 2006). The ability to collect our own in situ data is not within the scope of this project hence all in situ data is provided and collated externally (See Chapter 3 for complete description), and as a result, the use of validating in situ AOPs was not able to be incorporated.

5.2 Statistical Performance of products

The use of in situ data match-ups and subsequent performance metrics indicated that across oligotrophic, eutrophic, and overall, the regionally tuned Sentinel-3 product produced the lowest MAE scores, indicating the best overall accuracy; however, it contained the highest deviations from unity in terms of bias, showing a clear systematic error.

Whilst the performance of these two metrics might be assumed to be related, they function quite differently. The lack of absolute values within the bias equation (Equation 3.1), means that match-ups with both underestimations and overestimations can compensate for each other, driving the bias closer to unity. MAE

however, through the absolute value of the difference (Equation 3.2), penalises both underestimations and overestimations to the same degree. Bias is strictly a measure of systematic error, in that it requires the nature of the error to remain consistent to be revealed in the statistic. MAE accounts for stochastic error as well as precision, rewarding models which vary the least from the observed values.

GlobColour showed the lowest bias among all products, but the highest MAE values and most scatter around the 1:1 line. These results can be expected for an interpolated product (although interpolated results were removed through mask identification in our analysis), as they rely on substituting values in place of missing ones.

The performance of the global products in oligotrophic and mesotrophic conditions goes against what is perhaps commonly expected. The predominant use of Case-1 water algorithms within both global datasets tends to hinder their performance in more optically complex waters (Pramlall et al., 2023). However, despite high chl-a concentrations, the Southern Benguela does not typically experience high levels of turbidity from inorganic component backscattering. This could explain the improved performance of all three products in mesotrophic conditions. The influence of the in situ data set and sample size cannot be ignored, samples collected in different sites with different conditions could be prone to inconsistencies. Additionally, both the OC-CCI and GlobColour products produced < 30 match-ups in oligotrophic conditions and all three products produces < 30 match-ups in eutrophic conditions, which requires these specific results to be interpreted with a higher level of scrutiny. In comparison, previous studies have found that Case-1 algorithms used in both global products do not perform well in estimating higher biomass waters (Matthews et al., 2012; Smith et al., 2018).

All three products show poorer performance in eutrophic conditions, however the Sentinel-3 product far outperforms both the OC-CCI and GlobColour in terms of accuracy metrics, as expected, due to it's inclusion of the G2B algorithm to handle high chl-a concentration cases. OC-CCI performs the poorest in eutrophic conditions out of all three products yet simultaneously has the lowest MAE value of any product in mesotrophic conditions. This indicates that although it does not capture high biomass blooms accurately, it estimates chl-a values closest to in situ in more general conditions.

5.3 Comparison to previous studies

The bias metric used in ocean colour studies is often consistently represented by the same formula and doesn't often feature alternatives, allowing relatively simple comparison between different studies. However, direct comparisons to the accuracy metrics used in other studies would not have been possible without the inclusion of RMSE (due to it's common use). That being said, the indirect comparison of accuracy through the assessment of model-to-model performance can still be done; for example by assessing whether the same pattern of product performance appears in both studies.

Moradi (2021) used a different variant of GlobColour, better adapted to Case-2 waters (CHL2). This study found higher values of bias and overestimation in both their global products, however comparisons to this study break down quickly due to differences in the single sensor algorithms used, as well as the differing optical properties of the Benguela and Persian Gulf. Moradi (2021) found higher RMSE values when analysing OC-CCI in their study region (0.44 vs 0.37 in all samples). Overestimation of optically complex waters is a common issue for products built for Case-1 waters, it has been historically documented (Siegel et al., 2000) and is observed in many regional studies analysing global datasets (Moradi, 2021; Moradi and Zoljoodi, 2023; Sá et al., 2015). In contrast to these studies, the global datasets consistently underestimate chl-a in the Southern Benguela's most eutrophic conditions, highlighting the spectral differences between the Southern Benguela and 'typical' Case-2 water. Moradi and Zoljoodi (2023) found OC-CCI performed closer to in situ data than the GlobColour variant tested, which agreed with results found in this study. Additionally, OC-CCI outperformed other single sensor algorithms used in their study, with the exception of OC5.

Pramlall et al. (2023) used both GlobColour and OC-CCI in their evaluation of the British Columbia coastal waters. Measures of Bias for both products were similar to those showed in this study, with overall underestimations and a slightly stronger underestimation by the OC-CCI product. They found that OC-CCI performed better in terms of accuracy metrics across all conditions in comparison to the GlobColour product, which agrees with the results found in this study. They also found significantly lower RMSE values in comparison to those found in this study for both OC-CCI (0.25 vs 0.37) and GlobColour (0.28 vs 0.58).

Sá et al. (2015) tested OC-CCI against a suite of single sensor and algorithm combinations off Western Iberia. Whilst the OC-CCI outperformed certain MERIS algorithms, it showed consistent overestimation in the bias as well as higher RMSE values compared to the more regionally adapted algorithms. These bias results stand in contrast to those found in this study, with OC-CCI having an overall underestimation and stronger underestimations associated with higher chl-a concentrations.

5.4 The effects of match-up criteria, data processing and spatial scale

Despite an exhaustive attempt to retrieve appropriate chl-a data points for validation, the particular validation criteria for ocean colour data left 79, 112 and 114 valid match-ups out of an original 832 data points for the OC-CCI, GlobColour and Sentinel products respectively, with only 4 match-ups shared for all three products. Shared match-ups are ultimately far more desirable, as they allow for the direct comparison against a common set of in situ characteristics. Whilst all three products were run against the same sets of in situ data, they resulted in almost entirely different sets of match-ups.

This could be a result of the removal of non-unique pixels within the analysis step (See 3.2.1). While this step is applied independently to each product, the initial pixel used could vary from product to product,

with the 3x3 megapixel removing all other in situ match-ups in close vicinity. This effect can be seen in the number of pixels lost due to non-unique removal. The global products which feature 4 km resolution, both have their number of match-ups reduced by almost half when this validation step is applied. The Sentinel-3 product however, features 300 m resolution and hence only loses a marginal amount of match-ups through the removal on non-unique pixels. A potential work-around that might allow for more agreed match-ups is the use of only a single pixel for low resolution products as done in Pramlall et al. (2023), in favour of the 3x3 box used in this study.

The dissimilarity in the number of match-ups between data products is also likely a consequence of differences in their data processing. Since this study requires the comparison of two global datasets with markedly different merging, flagging and correction techniques (See 3.1.2), as well as a single instrument product, there are likely to be differences in the resulting data output values and presence/absence thereof. We can see evidence of this in Fig 4.6a, where masking and flagging techniques have removed many near-land pixels from the OC-CCI product.

When all match-ups are subset by those OC-CCI deemed valid, there are substantially lower numbers for both Sentinel and GlobColour. Since both global products use an almost identical list of sensors, and all products share OLCI data from 2016-onwards, the differences in swath should not greatly influence the number of match-ups between the global products. Additionally, the similarities between algorithms in the two global datasets also indicates these are not likely the reason for match-up quantity difference. The greatest factor contributing to these differences in match-ups is likely a combination the OC-CCI's pixel identification, quality flags and atmospheric correction techniques. Other studies directly comparing the two datasets within a regional context, have reached similar conclusions on the source of mismatch (Pramlall et al., 2023; Moradi, 2021, 2022).

Two visual groups of data points are removed after the OC-CCI subsetting. The Saldanha Bay points are likely removed due to being flagged as a bright-pixel or as sun glint, since they are in close proximity to the shoreline. The second group points were located in the open ocean, south of False bay, and hence are likely results of cloud pixel identification schemes. When comparing the case study visuals, the difference in flagging and merging techniques becomes even more obvious. The OC-CCI data set flags and masks many more pixels close to and adjacent to land. There are also some open ocean flag differences when compared to the Sentinel-3 dataset. GlobColour's gap free procedure is clearly noticeable on the 24th of February 2022; (Fig 4.6), even after removing interpolation flagged points, the product contains far more valid pixels in what appears to be a cloud covered day in the northern sections of the image.

The effects of the OC-CCI subsetting need to be interpreted with sufficient context. Since it involves the removing of OC-CCI invalids, it can be interpreted as a partial and imperfect application of the OC-CCI's processing mechanisms onto the other products. Imperfect due to the invalids potentially being a result of other issues such as swath cover or algorithm failure, and partial because elements of flagging protocols can

also result in changes to chl-a values (such as aerosol flagging and the subsequent atmospheric correction applied to reflectance) which would not be picked up by the subsetting.

The trade-off between number of valid pixels and performance is ultimately unavoidable. A more stringent pixel flagging scheme will leave better quality pixels and likely result in better estimates of chl-a and better algorithm performance, but will also remove more pixels from the retrieval, leaving fewer valids and more gaps. This can be seen in the example of Sentinel-3's results from all match-ups compared to its OC-CCI subset. The influence of the OC-CCI subsetting greatly reduces both the Sentinel-3's bias and MAE indicating either a) the removal of slightly erroneous pixels or b) the removal of particular conditions which the regional chl-a switching algorithm (Smith et al., 2018) struggles to estimate. However the OC-CCI product also has noticeably fewer match-ups (79), even when compared to the Sentinel-3 product (114), which is only able to utilize in situ data points from 2016-2024, 14 fewer years than the scope of in situ data available to the OC-CCI (Tables 3.2 and 4.1). These differences indicate the loss of available valid pixels, as a result of the stringent pixel flagging scheme the OC-CCI uses.

The collection of more spatially and temporally diverse chl-a data within the study region would help build more consistent results and allow for other metrics such as point-by-point accuracy to be applied.

5.5 Considerations for product application

Ocean Colour research can be used for numerous different practical applications, the requirements of which can help define and narrow down which products are used. Climate science for example would require robust products with long temporal coverage to allow for stable measurements and detect long-term climate trends. Models or research that use chl-a as an input or environmental variable, but don't require long term data may prioritise a product that can produce the most accurate results, in an attempt to best represent the in situ conditions. There are other more specific applications, such as warning systems for HAB's which would require NRT data, or phenology studies which would require a product that can handle high biomass chl-a concentrations and potentially inorganic material backscatter. Studies aiming to use satellite data for small scale regions would likely need to prioritise products with higher spatial resolution to better capture the mesoscale (or smaller) features needed.

The application of the products in this study within the St Helena bay region confirmed the results from the scatter plot analysis of in situ vs modelled response. Specifically, that the global products are under-estimating high chl-a concentrations whilst the Sentinel product is slightly overestimating. These results are repeated in the time series analysis and the significant differences in the peak average values across the products. The maximum chl-a zones displayed by the sentinel product are also spatially mismatched to the maximums displayed by the global datasets. Disagreements in maximum chl-a concentrations between products can be split into two separate issues. Systematic under or overestimation by a product will result in

different retrieved chl-a concentration values, and these will often be a result of certain algorithmic tunings, such as the choice of in water algorithms and their parameters. In these scenarios we would expect to see the same or similar visual patterns of chl-a but at different magnitudes i.e the products should still agree with the location of high and low chl-a but differ in their estimate values. The second more broad issue is differences in the processing chain, steps such as choice of atmospheric correction algorithms, flagging thresholds and masking techniques. These differences are more likely to cause spatial mismatch in the pattern of chl-a concentrations, something observed in the case study application. The findings suggest that there is some inherent process within the global datasets that breaks down in use or simply fails when receiving visual signals for high chl-a regions.

Whilst this may not be of large concern in application to open ocean regions (which almost never reach close to these chl-a concentrations), it raises some issues in coastal application. In many coastal scenarios, high biomass blooms are exactly the conditions attempting to be recorded and tracked using satellite remote sensing. Tracking high biomass blooms is critical for HAB detection, monitoring environmental health, public services, fisheries and potentially tourism if popular beaches are affected. In some of these scenarios, the detection is the only important metric. In these cases, the ability to detect any significant increase in chl-a will be useful to authorities. However there are other cases where the quantitative increase of chl-a is also relevant, such as phenological studies, or applications which use chl-a as an input variable for modelling.

Based on the limited cases seen here, a tentative approach would suggest global datasets such as OC-CCI and GlobColour begin to fail at estimations of chl-a concentrations higher than 30-50 mg m^{-3}, and therefore their use should be kept to regions that experience the lower end of eutrophic conditions. We acknowledge these are often fringe cases, but can be increasingly important when the implications of very high biomass blooms (such as hypoxic effects) become relevant (Pitcher and Nelson, 2006). The much higher spatial resolution offered by Sentinel-3 ocean colour products allows for the detection of finer-scale features in the coastal environment. Despite the lack of gap-free data, the higher resolution can- in some cases - allow for identification of high chl-a concentrations where lower resolution would have simply been flagged. This can be directly observed in the visual plots of the 24th of February, 2022 (Fig 4.6). A comparison of OC-CCI and Sentinel-3 on the same date reveals a similar gap of valid pixels within the clouded pixels. The OC-CCI's resolution only allows a few retrieved pixels with chl-a concentrations in the region of 10 mg m^{-3}. The Sentinel-3 product's resolution allows a much more detailed view of this gap in cloud cover, and within the many retrieved pixels, an identification of a high biomass bloom with chl-a concentrations above 250 mg m^{-3}. The combination of high spatial resolution, as well as an algorithm better adapted to resolve wide ranges of chl-a concentration, allows for the Sentinel-3 product to perform significantly better at identifying and estimating high biomass blooms.

There are drawbacks to higher resolution data however, many users and projects that work with datasets such as the OC-CCI require long term and potentially global scale. These constraints are confounded when multiple datasets are required or used for comparison. The 300 m resolution offered by the Sentinel-3 product

requires vastly stronger computational power and might pose practical issues when used in periods longer than a couple of years or larger regional scales. It's for these exact reasons, products such as OC-CCI are produced on monthly and weekly scales in addition to the daily scale applied for this study. Additionally, since the Sentinel-3 product is a single sensor product, it's temporal coverage only extends from 2016 onwards, when the OLCI instrument was operational. This stands in contrast to both merged datasets which cover an extensive period from 1997 to the present.

Temporal resolution may seem like a tempting solution for reducing computational power, but must be approached with caution when dealing with coastal zones. Coastal zones, and particularly those with upwelling features have been shown to have extreme short-term variability in productivity and chl-a (Jönsson et al., 2023b). Generally the concept of satellite validation and match-ups is to attempt to match and fall within the temporal variability of the in situ data itself. Using monthly estimates in a region such as the Benguela is sure to fail to represent the shorter term productivity features which commonly occur within it, particularly due to the pulsed nature of upwelling within this region. Ferreira et al. (2021) for example, studied the phenology of the Western Iberian Coast, a regional coastal area, using the daily OC-CCI product, and found the higher temporal resolution allowed for the detection of differences in bloom timing and duration; highlighting the importance of using a higher temporal resolution to assess phenological patterns in coastal regions.

Whilst the performance metrics indicate OC-CCI has a slightly lower MAE, the time-series plots show that GlobColour may better identify high biomass blooms in comparison to OC-CCI, indicating it may be the more appropriate product for use in phenological studies in coastal regions such as the Benguela. Additionally, from an operational perspective, the OC-CCI's lack of near-real time (NRT) data excludes it as a viable product for HAB detection systems, whilst GlobColour does provide a NRT service.

Global biogeochemical models, attempt to explain the biological, physical and chemical processes that occur and interact within the global ocean. These models require validation datasets to compare model vs observed responses and detail better configuration. Jönsson et al. (2023a) used OC-CCI data as an additional measure of comparison in conjunction to in situ measurements to better diagnose the performance of a physical–biogeochemical model (Darwin-CBIOMES-0). However, potential disagreement between satellite and in situ data particularly in coastal regions could lead to confusion and mismatch between the goal 'truth' value, and the validation set being used. The results of this study indicate that regionally tuned algorithms and datasets can better represent and estimate chl-a within coastal regions. In cases where satellite-derived data is used for the regional validation of biogeochemical models, global datasets should be examined with care and the pay-off of global coverage considered against a potentially substandard level of coastal chl-a estimation.

Similarly, chl-a values can be used as inputs to Net Primary Production (NPP) models such as the Eppley Vertically Generalized Production Model (Eppley-VGPM).Ryan-Keogh et al. (2025) used 6 different NPP

models to rank the accuracy of 15 different earth system models, in doing so, they used OC-CCI ocean colour data re-gridded to 25 km spatial resolution and 8-day temporal resolution as an input of chl-a concentration. Since NPP is a direct function of productivity, regions which feature higher productivity will contribute disproportionally compared to regions of lower productivity such as open ocean. These high productivity regions will also feature high chl-a concentrations due to the large quantity of phytoplankton. Future applications of global NPP budgets would benefit from the inclusion of regional chl-a algorithms such as the Sentinel-3 algorithm used in this study, as to more accurately quantify regions of high productivity, as well as to increase the capability of capturing high biomass bloom events, which are useful contributions in determining NPP.

Chapter 6

Conclusions

The results of this study evaluate the performance of CMEMS GlobColour and OC-CCI version 6 chl-a products and compares their statistical metrics against that of regionally developed Sentinel-3 algorithm output. Although the Sentinel-3 product showed the closest results to in situ data of all three products, it was found to have a consistent overestimation bias. Both merged products underestimated high chl-a concentrations and overestimated low chl-a concentrations. A case study within the St. Helena Bay region showed that the Sentinel-3's chl-a product is able to identify very high biomass blooms whilst both merged products failed to capture the intense chl-a peaks expected in this region. Event-scale analysis showed the strong effects of flagging and processing differences between the merged products, with the Globcolour product showing greater ability to capture bloom timing and variability than OC-CCI. OC-CCI's more stringent flagging results in fewer pixel retrievals but better scoring performance metrics, particularly in mesotrophic conditions between 1 and 15 mg m^{-3}. Comparison with more optically turbid regional studies found contrasting results, highlighting the Southern Benguela's unique optical properties, whereas comparisons with other similar regional coasts found agreement in merged product performance.

Bibliography

Bailey, S. W. and Werdell, P. J. (2006). A multi-sensor approach for the on-orbit validation of ocean color satellite data products. *Remote Sensing of Environment* 102, 12–23. doi:10.1016/J.RSE.2006.01.015

Bernard, S., Probyn, T. A., and Barlow, R. G. (2001). Measured and modelled optical properties of particulate matter in the southern benguela. *South African Journal of Science* 97, 410–420

Brewin, R. J., Sathyendranath, S., Müller, D., Brockmann, C., Deschamps, P. Y., Devred, E., et al. (2015). The ocean colour climate change initiative: Iii. a round-robin comparison on in-water bio-optical algorithms. *Remote Sensing of Environment* 162, 271–294. doi:10.1016/J.RSE.2013.09.016

Collins, S., Rost, B., and Rynearson, T. A. (2014). Evolutionary potential of marine phytoplankton under ocean acidification. *Evolutionary Applications* 7, 140–155. doi:10.1111/EVA.12120

Couto, A. B., Brotas, V., Mélin, F., Groom, S., and Sathyendranath, S. (2016). Inter-comparison of oc-cci chlorophyll-a estimates with precursor data sets. *International Journal of Remote Sensing* 37, 4337–4355. doi:10.1080/01431161.2016.1209313

[Dataset] de Villiers, S. (2017). Seawater biogeochemical measurements (nutrients, chlorophyll-a and pCO2) from high-resolution underway sampling across the Agulhas Bank in 2014 and 2015. doi: 10.1594/PANGAEA.882181

Demarcq, H., Barlow, R., Hutchings, . L., and Hutchings, L. (2007). Application of a chlorophyll index derived from satellite data to investigate the variability of phytoplankton in the benguela ecosystem. *African Journal of Marine Science* 29, 1814–2338. doi:10.2989/A

Demarcq, H., Barlow, R. G., and Shillington, F. A. (2003). Climatology and variability of sea surface temperature and surface chlorophyll in the benguela and agulhas ecosystems as observed by satellite imagery. *African Journal of Marine Science* 25, 363–372. doi:10.2989/18142320309504022

Felden, J., Möller, L., Schindler, U., Huber, R., Schumacher, S., Koppe, R., et al. (2023). Pangaea - data publisher for earth environmental science. *Scientific Data* 10. doi:10.1038/s41597-023-02269-x

Ferreira, A., Brotas, V., Palma, C., Borges, C., and Brito, A. C. (2021). Assessing phytoplankton bloom phenology in upwelling-influenced regions using ocean color remote sensing. *Remote Sensing* 13, 1–27. doi:10.3390/rs13040675

Field, C. B., Behrenfeld, M. J., Randerson, J. T., and Falkowski, P. (1998). Primary production of the biosphere: integrating terrestrial and oceanic components. *Science* 281, 237–240

Garnesson, P., Mangin, A., D'Andon, O. F., Demaria, J., and Bretagnon, M. (2019). The cmems globcolour chlorophyll a product based on satellite observation: Multi-sensor merging and flagging strategies. *Ocean Science* 15, 819–830. doi:10.5194/os-15-819-2019

Gitelson, A. A., Zhou, J., Gurlin, D., Moses, W., Ioannou, I., Ahmed, S. A., et al. (2010). Algorithms for remote estimation of chlorophyll-a in coastal and inland waters using red and near infrared bands. *Optics Express* 18

Gohin, F., Druon, J. N., and Lampert, L. (2002). A five channel chlorophyll concentration algorithm applied to sea wifs data processed by seadas in coastal waters. *International Journal of Remote Sensing* 23, 1639–1661. doi:10.1080/01431160110071879

Gordon, H. R., Clark, D. K., Mueller, J. L., and Hovis, W. A. (1980). Phytoplankton pigments from the nimbus-7 coastal zone color scanner: Comparisons with surface measurements. *Science* 210, 63–66

Gower, J. F., Doerffer, R., and Borstad, G. A. (1999). Interpretation of the 685nm peak in water-leaving radiance spectra in terms of fluorescence, absorption and scattering, and its observation by meris. *International Journal of Remote Sensing* 20, 1771–1786. doi:10.1080/014311699212470

Gregg, W. W. and Woodward, R. H. (1998). Communications improvements in coverage frequency of ocean color: Combining data from seawifs and modis. *IEEE transactions on Geoscience and Remote Sensing* 36, 1350–1353

Grémillet, D., Lewis, S., Drapeau, L., Lingen, C. D. V. D., Huggett, J. A., Coetzee, J. C., et al. (2008). Spatial match-mismatch in the benguela upwelling zone: Should we expect chlorophyll and sea-surface temperature to predict marine predator distributions? *Journal of Applied Ecology* 45, 610–621. doi: 10.1111/j.1365-2664.2007.01447.x

Hoyer, S. and Hamman, J. (2017). xarray: N-d labeled arrays and datasets in python. *Journal of Open Research Software* 5, 10. doi:10.5334/jors.148

Hu, C., Lee, Z., and Franz, B. (2012). Chlorophyll a algorithms for oligotrophic oceans: A novel approach based on three-band reflectance difference. *Journal of Geophysical Research: Oceans* 117. doi:10.1029/2011JC007395

Hutchings, L., van der Lingen, C. D., Shannon, L. J., Crawford, R. J., Verheye, H. M., Bartholomae, C. H., et al. (2009). The benguela current: An ecosystem of four components. *Progress in Oceanography* 83, 15–32. doi:10.1016/j.pocean.2009.07.046

IOCCG (2000). Remote Sensing of Ocean Colour in Coastal, and Other Optically-Complex, Waters. In *Reports of the International Ocean-Colour Coordinating Group, No. 3*, ed. S. Sathyendranath (IOCCG, Dartmouth, Canada)

IOCCG (2007). Ocean-Colour Data Merging. In *Reports of the International Ocean-Colour Coordinating Group, No. 6*, ed. W. Gregg (IOCCG, Dartmouth, Canada)

[Dataset] Jackson, T., Sathyendranath, S., Groom, S., and Calton, B. (2022). Esa ocean colour climate change initiative-phase 3 product user guide for v6.0 dataset

Jönsson, B. F., Follett, C. L., Bien, J., Dutkiewicz, S., Hyun, S., Kulk, G., et al. (2023a). Using probability density functions to evaluate models (pdfem, v1.0) to compare a biogeochemical model with satellite-derived chlorophyll. *Geoscientific Model Development* 16, 4639–4657. doi:10.5194/gmd-16-4639-2023

Jönsson, B. F., Salisbury, J., Atwood, E. C., Sathyendranath, S., and Mahadevan, A. (2023b). Dominant timescales of variability in global satellite chlorophyll and sst revealed with a moving standard deviation saturation (moss) approach. *Remote Sensing of Environment* 286, 113404. doi:10.1016/J.RSE.2022.113404

Lain, L. R., Bernard, S., and Evers-King, H. (2014). Biophysical modelling of phytoplankton communities from first principles using two-layered spheres: Equivalent algal populations (eap) model. *Optics Express* 22, 16745. doi:10.1364/oe.22.016745

Lamont, T., Brewin, R. J., and Barlow, R. G. (2018). Seasonal variation in remotely-sensed phytoplankton size structure around southern africa. *Remote Sensing of Environment* 204, 617–631. doi:10.1016/j.rse.2017.09.038

Lee, Z., Carder, K. L., and Arnone, R. A. (2002). Deriving inherent optical properties from water color: a multiband quasi-analytical algorithm for optically deep waters. *Applied Optics* 41, 5755. doi:10.1364/ao.41.005755

[Dataset] Lee, Z., Lubac, B., Werdell, J., and Arnone, R. (2009). An update of the quasi-analytical algorithm (qaa_v5)

Mason, P., Zillman, J., Simmons, A., Lindstrom, E., Harrison, D., Dolman, H. A., et al. (2010). Implementation plan for the global observing system for climate in support of the unfccc (2010 update). *Word Meteorological Organization (WMO)*

Matthews, M. W., Bernard, S., and Robertson, L. (2012). An algorithm for detecting trophic status (chlorophyll-a), cyanobacterial-dominance, surface scums and floating vegetation in inland and coastal waters. *Remote Sensing of Environment* 124, 637–652. doi:10.1016/J.RSE.2012.05.032

[Dataset] Mbelengwa, P. (2023). West coast rock lobster contingency plan activated following marine species walkouts

McClain, C. R., Feldman, G. C., and Hooker, S. B. (2004). An overview of the seawifs project and strategies for producing a climate research quality global ocean bio-optical time series. *Deep-Sea Research Part II: Topical Studies in Oceanography* 51, 5–42. doi:10.1016/j.dsr2.2003.11.001

McKinney, W. et al. (2010). Data structures for statistical computing in python. In *Proceedings of the 9th Python in Science Conference* (Austin, TX), vol. 445, 51–56

Mobley, C. D. (2022). *The Oceanic Optics Book* (International Ocean Colour Coordinating Group (IOCCG)). doi:10.25607/OBP-1710

Moore, C. M., Mills, M. M., Arrigo, K. R., Berman-Frank, I., Bopp, L., Boyd, P. W., et al. (2013). Processes and patterns of oceanic nutrient limitation. *Nature Geoscience* 6, 701–710. doi:10.1038/ngeo1765

Moore, T. S., Campbell, J. W., and Dowell, M. D. (2009). A class-based approach to characterizing and mapping the uncertainty of the modis ocean chlorophyll product. *Remote Sensing of Environment* 113, 2424–2430. doi:10.1016/j.rse.2009.07.016

Moradi, M. (2021). Evaluation of merged multi-sensor ocean-color chlorophyll products in the northern persian gulf. *Continental Shelf Research* 221. doi:10.1016/j.csr.2021.104415

Moradi, M. (2022). Inter-comparison of single-sensor and merged multi-sensor ocean color chlorophyll-a products in the shallow turbid waters-case study: Persian gulf. *International Journal Of Coastal, Offshore And Environmental Engineering (ijcoe)* 7, 1–10

Moradi, M. and Zoljoodi, M. (2023). Validation of standard ocean-color chlorophyll-a products in turbid coastal waters: A case study on statistical evaluation and quality control tests in the persian gulf. *Journal of Marine Systems* 240. doi:10.1016/j.jmarsys.2023.103875

Morel, A. Y. and Gordon, H. R. (1983). *Remote Assessment of Ocean Color for Interpretation of Satellite Visible Imagery* (Springer-Verlag)

Ndhlovu, A., Dhar, N., Garg, N., Xuma, T., Pitcher, G. C., Sym, S. D., et al. (2017). A red tide forming dinoflagellate prorocentrum triestinum: identification, phylogeny and impacts on st helena bay, south africa. *Phycologia* 56, 649–665. doi:10.2216/16-114.1

Nechad, B., Ruddick, K., Schroeder, T., Oubelkheir, K., Blondeau-Patissier, D., Cherukuru, N., et al. (2015). Coastcolour round robin data sets: A database to evaluate the performance of algorithms for the retrieval of water quality parameters in coastal waters. *Earth System Science Data* 7, 319–348. doi:10.5194/essd-7-319-2015

O'Reilly, J. E. and Werdell, P. J. (2019). Chlorophyll algorithms for ocean color sensors - OC4, OC5 OC6. *Remote Sensing of Environment* 229, 32–47. doi:10.1016/j.rse.2019.04.021

[Dataset] Pardo, S., Tilstone, G. H., Dall'olmo, G., Jordan, T. M., Brewin, R. J. W., and Casal, T. G. D. (2024). Global assessment of merged multi-sensor ocean colour chlorophyll a products

Pitcher, G. C. and Nelson, G. (2006). Characteristics of the surface boundary layer important to the development of red tide on the southern namaqua shelf of the benguela upwelling system. *Limnol. Oceanogr* 6, 2660–2674. doi:10.2307/4499646

Pitcher, G. C. and Probyn, T. A. (2016). Suffocating phytoplankton, suffocating waters-red tides and anoxia. *Frontiers in Marine Science* 3. doi:10.3389/fmars.2016.00186

Pramlall, S., Jackson, J. M., Konik, M., and Costa, M. (2023). Merged multi-sensor ocean colour chlorophyll product evaluation for the british columbia coast. *Remote Sensing* 15. doi:10.3390/rs15030687

Redfield, A. C. (1958). The biological control of chemical factors in the environment. *American Scientist* 46, 205–221

Ryan-Keogh, T. J., Tagliabue, A., and Thomalla, S. J. (2025). Global decline in net primary production underestimated by climate models. *Communications Earth Environment* 6, 75. doi:10.1038/s43247-025-02051-4

Salomonson, V. V., Barnes, W. L., Maymon, P. W., Montgomery, H. E., and Ostrow, H. (1989). Modis: advanced facility instrument for studies of the earth as a system. *IEEE Transactions on Geoscience and Remote Sensing* 27, 145–153. doi:10.1109/36.20292

Sathyendranath, S., Brewin, R. J., Brockmann, C., Brotas, V., Calton, B., Chuprin, A., et al. (2019). An ocean-colour time series for use in climate studies: The experience of the ocean-colour climate change initiative (oc-cci). *Sensors (Switzerland)* 19. doi:10.3390/s19194285

Seegers, B. N., Stumpf, R. P., Schaeffer, B. A., Loftin, K. A., and Werdell, P. J. (2018). Performance metrics for the assessment of satellite data products: an ocean color case study. *Optics Express* 26, 7404. doi:10.1364/oe.26.007404

Shannon, L. V., Schlittenhardt, P., and Mostert, S. A. (1984). The nimbus 7 czcs experiment in the benguela current region off southern africa, february 1980: 2. interpretation of imagery and oceanographic implications. *Journal of Geophysical Research* 89, 4968–4976. doi:10.1029/JD089iD04p04968

Siegel, D. A., Wang, M., Maritorena, S., Robinson, W., Arnone, B., and Stumpf, R. (2000). Atmospheric correction of satellite ocean color imagery: The black pixel assumption. *Applied Optics* , 1–36

[Dataset] Smith, M. (2024). Olci_300m_wcp_chla. doi:10.5281/zenodo.13927326

[Dataset] Smith, M. (2025). Surface chlorophyll a concentration and secchi depth data from the seahab project, march 2023. doi:10.15493/DEA.MIMS.14512023

Smith, M. E., Lain, L. R., and Bernard, S. (2018). An optimized chlorophyll a switching algorithm for meris and olci in phytoplankton-dominated waters. *Remote Sensing of Environment* 215, 217–227. doi:10.1016/j.rse.2018.06.002

Steinmetz, F., Deschamps, P.-Y., and Ramon, D. (2011). Atmospheric correction in presence of sun glint: application to meris. *Optics Express* 19, 9783–9800

Sá, C., D'Alimonte, D., Brito, A. C., Kajiyama, T., Mendes, C. R., Vitorino, J., et al. (2015). Validation of standard and alternative satellite ocean-color chlorophyll products off western iberia. *Remote Sensing of Environment* 168, 403–419. doi:10.1016/J.RSE.2015.07.018

Valente, A., Sathyendranath, S., Brotas, V., Groom, S., Grant, M., Jackson, T., et al. (2022). A compilation of global bio-optical in situ data for ocean colour satellite applications – version three. *Earth System Science Data* 14, 5737–5770. doi:10.5194/essd-14-5737-2022

van der Lingen, C. D., Hutchings, L., Lamont, T., and Pitcher, G. C. (2016). Climate change, dinoflagellate blooms and sardine in the southern benguela current large marine ecosystem. *Environmental Development* 17, 230–243. doi:10.1016/j.envdev.2015.09.004

van Oostende, M., Hieronymi, M., Krasemann, H., and Baschek, B. (2023). Global ocean colour trends in biogeochemical provinces. *Frontiers in Marine Science* 10. doi:10.3389/fmars.2023.1052166

Villiers, S. D. (1998). Seasonal and interannual variability in phytoplankton biomass on the southern african continental shelf: Evidence from satellite-derived pigment concentrations. *South African Journal of Marine Science* , 169–179doi:10.2989/025776198784126872

Weeks, S. J. (2004). *Specific Applications of Satellite Remote Sensing to the Benguela Ecosystem.* Ph.D. thesis, University of Cape Town

Weeks, S. J., Barlow, R., Roy, C., and Shillington, F. A. (2006). Remotely sensed variability of temperature and chlorophyll in the southern benguela: Upwelling frequency and phytoplankton response. *African Journal of Marine Science* 28, 493–509. doi:10.2989/18142320609504201

Werdell, P. J. and Bailey, S. W. (2005). An improved in-situ bio-optical data set for ocean color algorithm development and satellite data product validation. *Remote Sensing of Environment* 98, 122–140. doi:10.1016/j.rse.2005.07.001

Werdell, P. J., Franz, B. A., Bailey, S. W., Feldman, G. C., Boss, E., Brando, V. E., et al. (2013). Generalized ocean color inversion model for retrieving marine inherent optical properties. *Applied optics* 52, 2019–2037

Yasunaka, S., Ono, T., Sasaoka, K., and Sato, K. (2022). Global distribution and variability of subsurface chlorophyll a concentrations. *Ocean Science* 18, 255–268. doi:10.5194/os-18-255-2022

Yu, S., Bai, Y., He, X., Gong, F., and Li, T. (2023). A new merged dataset of global ocean chlorophyll-a concentration for better trend detection. *Frontiers in Marine Science* 10. doi:10.3389/fmars.2023.1051619